Synthesis, Characterization and Applications of Transition Metal Chalcogenides and Transition Metal Dichalcogenide Nanostructures

Declaration

I hereby declare that the work which is presented in this thesis titled **"Synthesis, Characterization and Applications of Transition Metal Chalcogenides and Transition Metal Dichalcogenide Nanostructures"** has been carried out by me under the guidance of Dr. Sudhir Cherukulappurath at Department of Physics, Goa University. This work has not been submitted in part or full for a degree, diploma or fellowship to this/any other university or Institute. Wherever contributions of others are involved, every effort has been made to indicate this clearly with due acknowledgement. This thesis is a record of original work done by me and all sources listed within have been detailed in bibliography.

……………………………...

Ruchika Thayil

M.Sc. Physics

Department of Physics

Goa University

Acknowledgement

I would first like to thank my thesis advisor Dr. Sudhir Cherukulappurath of the School of Physical and Applied Sciences at Goa University. The door to Dr. Cherukulappurath's office was always open whenever I ran into a trouble spot or had a question about my research.

I would also like to thank Dr. Kaustubh R.S. Priolkar, Dr. Bholanath Pahari and Dr. Venkatesha R. Hathwar for the knowledge they have imparted to me.

I am deeply indebted to Mr. Praveenkumar Pinapati for the aspiring guidance and help provided.

Finally, I must express my very profound gratitude to my family for providing me with unfailing support and continuous encouragement.

Abstract

Nanostructured materials having a well defined size and shape have attracted much interest due to their great potential for fundamental research related to the effect of dimensionality and size on various physical and chemical properties. In this work, 3D Wurtzite Zinc Selenide (ZnSe) and various Molybdenum Dichalcogenide (MoX_2; X=S, Se, Te) nanostructures have been synthesized using the hydrothermal method. The samples were characterized by X-ray diffraction (XRD), Raman Spectroscopy, UV-Visible spectroscopy and scanning electron microscopy (SEM). Furthermore their application toward environmental remediation has been investigated. We have studied the degradation of common organic dyes such as methylene blue (MB), methyl orange (MO), malachite green (MG), rhodamine-B, rhodamine 6G and also the mixtures of these organic dyes which causes severe environmental contamination issues. It was observed that among the synthesized samples, Molybdenum disulfide (MoS_2) showed excellent catalytic activity in the degradation of all of these dyes. The application of Surface enhanced Raman scattering (SERS) in the detection of the degradation of the dyes in the experiments was also investigated.

Contents

CHAPTER-1

INTRODUCTION

1.Introduction

Chalcogenides such as sulfide, selenide and telluride based-compounds are abundant and their derivatives such as binary, ternary, and quaternary chalcogenide materials are widely used in areas such as photovoltaic, photocatalyst, sensor, fuel cell, and battery. Due to their own unique characteristics, structure, and physical as well as chemical properties they are one of the most studied nanostructures. These wide-band gap semiconductor materials have attracted considerable attention due to their size-dependent properties and potential for several technological applications [1]. In particular, nanostructured semiconductor materials having a well-defined size and shape have are of much interest due to their great potential for fundamental research related to effect of dimensionality and size on various physical and chemical properties as well as for its application in electronics and optoelectronic devices [2]. Among the various group II-VI semiconductors, ZnSe with a direct bandgap of 2.70 eV (460 nm) has attracted significant attention due to its applications in light emitting diodes (LEDs), biomedical sensors, photovoltaic solar cells and as photocatalysts [3]. ZnSe is also an excellent host for the formation of doped nanocrystals [4]. All kinds of synthesis methods including hydrothermal, chemical vapor deposition (CVD), sol-gel and solvothermal methods have been applied widely for the synthesis of ZnSe nanostructures with different morphologies [5]. In addition to this, many new methods have also been investigated to synthesize ZnSe which includes a variety of colloids and composite particles [6]. For example, Cao et al. reported a simple hydrothermal route for the synthesis of wurtzite 3D flower-like ZnSe nanostructures by a complex hydrothermal treatment using ethylenediamine- tetraacetic acid (EDTA) in which they showed that the addition of chelator EDTA played a critical role in the formation of 3D flowerlike ZnSe nanostructures. [7].

In this present work, ZnSe nanostructures were synthesized using a similar hydrothermal method by varying the concentration of EDTA. The energy band gap obtained from UV-Vis spectroscopy of ZnSe is found to be 2.75 eV from the Kubelka-Munk function. XRD patterns of samples were obtained in the angle range of 10°–70°, using Cu-Kα radiation (λ = 1.5406 Å).

All the diffraction peaks in the pattern can be indexed to Wurtzite (hexagonal) structure in accordance with the JCPDS card no.15-0105 for ZnSe. The Raman spectra were obtained using a LabRAM HR Evol Raman system with a 532 nm laser source. The Raman bands at 205 cm^{-1} and 251 cm^{-1} are attributed to the transverse-optic (TO) phononic mode and longitudinal-optic (LO) phononic modes. The Photoluminescence spectra was recorded using a Cary Eclipse fluorescence spectrophotometer. The emission band at 488 nm and 554 nm are usually assigned to self-activated luminescence resulting from donor-acceptor pairs that are related to Zn vacancy and interstitial states, or associated with surface emission. Photocatalytic experiments were carried out using ZnSe in the degradation of Rhodamine-B using UV source however, complete degradation was not observed.

Out of various class of materials ranging from bulk to nanoscale, transition metal dichalcogenides (TMDs) have gained popularity due to their excellent structural and physical features such as stability compositional flexibility, surface area, electronic conductivity, porosity and layered assemblies [8]. Two-dimensional transition metal dichalcogenides (2D-TMDs) have been explored worldwide due to their potential applications such as catalysis, energy storage, electronics, optoelectronics, photonics, gas sensors etc. TMDs have an X-M-X layer structure, so that its single layer includes a layer of molybdenum (M), which is between two layers of chalcogenide(X)[9].

Unlike graphene, TMDs having band gaps in the range of 1–2 eV, can be applied in solar cells and photodetectors [10]. They have also enabled the advances of electronic and sensor devices, catalytic characteristics as well as flexible devices because of their extraordinary properties arising from their direct band gaps, high on/off current ratio, and high mechanical flexibility [11, 12]. Different techniques such as RF magnetron sputtering, electron beam evaporation, chemical vapor deposition (CVD), spin coating, sol gel, and hydrothermal have been utilized to synthesize such nanostructures. The hydrothermal method is one of the most important techniques for advanced materials processing of various metal oxides and metal sulfides. The relative simplicity, easily achievable temperature conditions, large-scale generalizability, and cost-effectiveness are the key features of the hydrothermal method [13].

Molybdenum disulfide (MoS_2) is one among the most stable TMDs that can be synthesized. It is composed of layers in a trigonal prismatic arrangement involving an atomic plane of Mo sandwiched between two atomic planes of S. Here the MoS_2 layers are bound to each other by weak Van der Waals forces, while S and Mo atoms have strong covalent bonds between each other. In the MoS_2, the 2H phase, the Mo atom is surrounded in trigonal prismatic coordination with two S–Mo–S units per elemental cell [14]. Molybdenum selenide ($MoSe_2$) has also been extensively studied in recent years due to its strong absorption of sunlight and unique band structure while $MoTe_2$ is gaining interests in electronic and optoelectronic devices [15,16].

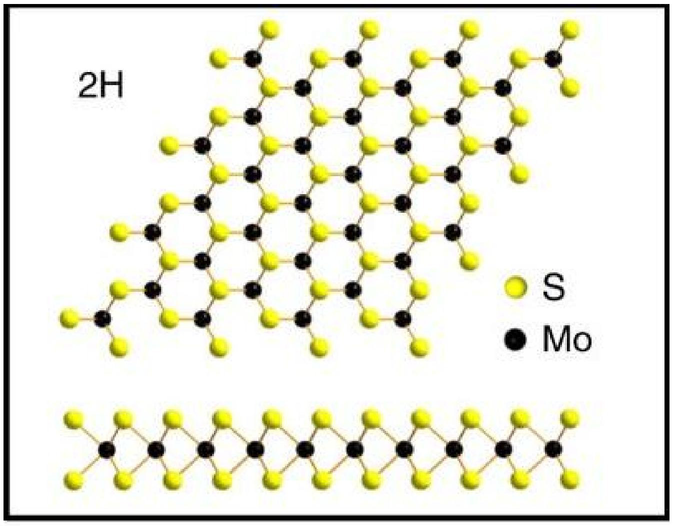

Fig.1. Schematic of 2H- MoS_2 structure (adapted from [24])

In this work, we have synthesized MoS_2, $MoSe_2$ and $MoTe_2$ using the hydrothermal method. The energy band gap from UV-Vis spectroscopy of MoS_2 is found to be 2.1eV. The X-ray diffraction pattern exhibited two main peaks at 33.20 ° and 57.23 ° which were attributed to the (100) and (110) peaks of 2H MoS_2 synthesized at 200°C whereas, the XRD pattern exhibited two additional peaks at 14.2° and 39.5° corresponding to (002) and (103) peaks of 2H MoS_2 when synthesized at 210° C. The appearance of two first-order Raman active modes of MoS_2, namely E_{2g} and A_{1g} at 380 cm^{-1} and 405 cm^{-1}, respectively, confirmed the formation of MoS2. The energy band gap from UV-Vis spectroscopy of $MoSe_2$ is found to be 1.55 eV. The Raman spectrum of $MoSe_2$ was recorded at room temperature with an excitation wavelength 532 nm. Peaks position at 287 cm^{-1} and 239 cm^{-1} correspond to that of 2H $MoSe_2$. It was observed that the order of crystallinity of $MoTe_2$ is much higher compared to MoS_2 and $MoSe_2$.

Environmental pollution has been an issue of great concern across the globe and the industrial effluents having various toxic and harmful chemicals including organic dyes are jeopardizing the natural resources. Also, most dyes are toxic and exhibit carcinogenic, mutagenic and teratogenic properties. Massey et al. have shown hierarchical microspheres of MoS_2 nanosheets are efficient and regenerative adsorbent for removal of methylene blue, malachite green, rhodamine 6G, fuchsin acid and congo red dyes and illustrated the kinetic study of methylene blue dye on to the MoS_2 nanosheets synthesized at 230°C [16]. Geng et al. synthesized the three-dimensional flower-like MoS_2 nanostructure and revealed as an adsorbent for cationic dye Rhodamine B and found that MO cannot be removed from water by the flower-like MoS_2 which preferentially adsorb the cationic dye (RhB) [18]. Wu et al. showed superior adsorption of methyl orange by h-MoS2 microspheres synthesized at 220°C [20].

In this work, MoS_2 synthesized at 200°C was found to be effective in the degradation of organic dyes such as methylene blue (MB), methyl orange (MO), malachite green (MG), rhodamine-B and rhodamine 6G. We have tested the adsorption properties of MoS_2 toward each of them in single and combined dye systems such as (MO+MB), (MB+MG) and (MB and RhB).
SERS studies in the detection of dye concentration after regular intervals of time were also performed.

1.1.Objectives

- To synthesize chalcogenide based cost-effective, recyclable catalyst for the degradation of organic dyes having high degradation efficiency without the aid of any light sources.

- In this work, 3D Wurtzite Zinc Selenide (ZnSe) and various Molybdenum Dichalcogenide (MoX_2; X=S, Se, Te) nanostructures have been synthesized using the hydrothermal method.

- MoS_2 shows remarkable degradation activity of various organic dyes such as MB, MO, MG, Rhodamine B, Rhodamine 6G, mixture of (MO+MB), (MB+MG) and mixture of (MB and RhB) dyes which causes severe environmental contamination issues.

- MoS_2 can be efficiently regenerated and reused for the dye adsorption without compromising the adsorption capacity.

- Application of Surface enhanced Raman scattering (SERS) in the detection of the degradation of the dyes in the experiments.

CHAPTER-2

SYNTHESIS METHODS

2.Synthesis methods

3D Wurtzite Zinc Selenide (ZnSe) and various Molybdenum Dichalcogenide (MoX_2; X=S, Se, Te) nanostructures were synthesized using the simple and cost-effective technique of hydrothermal synthesis. The hydrothermal method refers to the use of an aqueous solution as a reaction system which is added in a special close reaction vessel.

This creates a high-temperature, high pressure reaction environment by heating the reaction system and pressurizing it. This process dissolves and recrystallizes a substance which is otherwise poorly soluble or insoluble under normal conditions. The main steps of crystalline growth consist of dissolving the reactants in a hydrothermal medium which allows the formation of ions or molecules. These ions or molecules are separated by the temperature difference between the upper and lower portions of the kettle.

In a hydrothermal reaction, water can participate in the reaction as a chemical component, a solvent or a puffing accelerator. The ions or molecular groups are then transported to the low-temperature region, where the seed crystal is grown to form a supersaturated solution. Next, the ions or molecular groups are adsorbed, decomposed, and desorbed at the growth interface and the adsorbed material moves at the interface. The dissolved matter then crystallizes in the final step.[20]

Sample Preparation.

2.1. Hydrothermal Synthesis and Characterization of 3D Wurtzite ZnSe Nanostructures

All chemicals used in this experiment were of analytical grade. The preparation of ZnSe nanostructures was performed by a one-pot approach. Typically, 1.286 g of NaOH was dissolved in 32 mL of distilled water and then 0.248 g of $Zn(NO_3)2\cdot 6H_2O$ and 2.02 g of EDTA were added successively into the above solution. The resulting mixture was sonicated until a clear solution was obtained. Next, 0.182 g of Na_2SeO_3 and 16.2 mL of hydrazine hydrate $N_2H_4\cdot H_2O$ was sequentially added into this reaction. After the mixture was magnetic stirred for 10 min, the final solution was then transferred into a Teflon-lined autoclave of 100 mL capacity. After heating at 180 °C for 2 h, the tank was cooled down to room temperature naturally. Yellowish floccules of ZnSe crystals were formed in solution which was then treated with 1 M HCl solution. The resultant product was washed with distilled water and absolute ethanol and finally dried at 70 °C for 2 h. The process was repeated for an EDTA concentration of 1.05g.

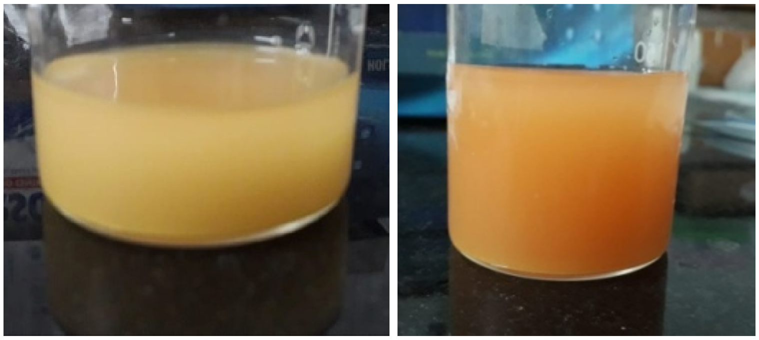

(a) (b)

Fig.2: Synthesis of ZnSe (a)Before adding 1 M HCl (b) After adding 1M HCl solution.

2.2. Molybdenum Dichalcogenide (MoX_2; X=S, Se, Te) nanostructures

Synthesis of MoS_2

A few layered MoS2 nanosheets were synthesized by a one-step hydrothermal reaction method. In a typical experiment, 1.288g Na_2MoO_4 (Sigma-Aldrich, 99%) and 1.906g thioacetamide (C2H5NS, Sigma-Aldrich, 99%) were dissolved in 80ml deionized (DI) water and stirred for 1 h at 27°C by using a magnetic stirrer. The solution was transferred to a 100 ml stainless steel autoclave, which was then heated up to 200°C and kept for 24 h. After cooling naturally, the product was filtered, washed with DI water followed by ethanol and dried at 70°C for 4 hours. MoS_2 was also synthesized at 210°C with precursor ratio 1:5.

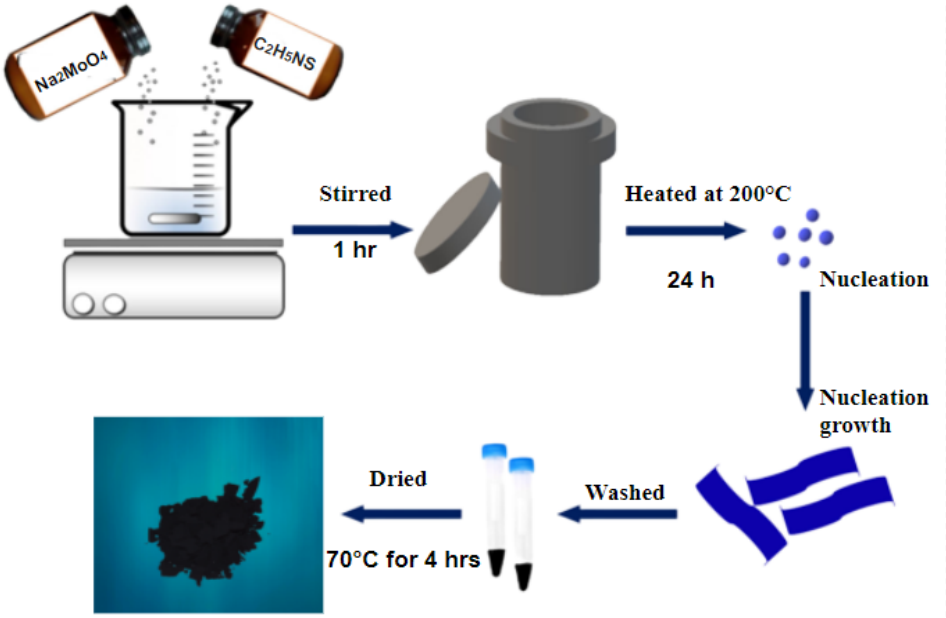

Fig.3: *Synthesis of* MoS_2

Synthesis of $MoSe_2$

In this method, Se nanoparticles were prepared by making an aq. stock solution of 100mM sodium selenite and 400 mM ascorbic acid. Ascorbic acid was added drop wise to the sodium selenite solution under magnetic stirring at 300 RPM at room temperature for 20 min. The mixtures were allowed to react till the color change was observed from colorless to orange. Soon after the change was observed the mixtures were diluted to 25 mL DI water and washed several times with DI water. These Se nanoparticles were used in the synthesis of MoSe2.The process involves formation of black solution by adding 0.25 g of Se nanoparticles, 0.1 g of sodium borohydride and 0.65 g of sodium molybdate in 40 mL of DI water at room temperature. The as-formed mixture was stirred for 10 min, ensuring the complete dispersion of Selenium and then transferred into the teflon-lined stainless-steel autoclave of 100mL capacity, sealed and placed in the oven at 200°C for 24 h. After the autoclave cooled down naturally, the precipitate was cooled by washing with excess DI water and dried at 50°C for 1 h.

Synthesis of $MoTe_2$

For the synthesis of $MoTe_2$ 1.45 g of sodium molybdate, 1.53 g of tellurium metal powder and 0.34 g of sodium borohydride was added in 80 mL of DI water at room temperature. The mixture was stirred for 10 min followed by transfer of mixture to teflon-lined stainless-steel autoclave and hydrothermal process at 200 °C for 48 hours. The sample was collected, washed with DI water followed by ethanol and finally dried at 60 °C for 2 hours.

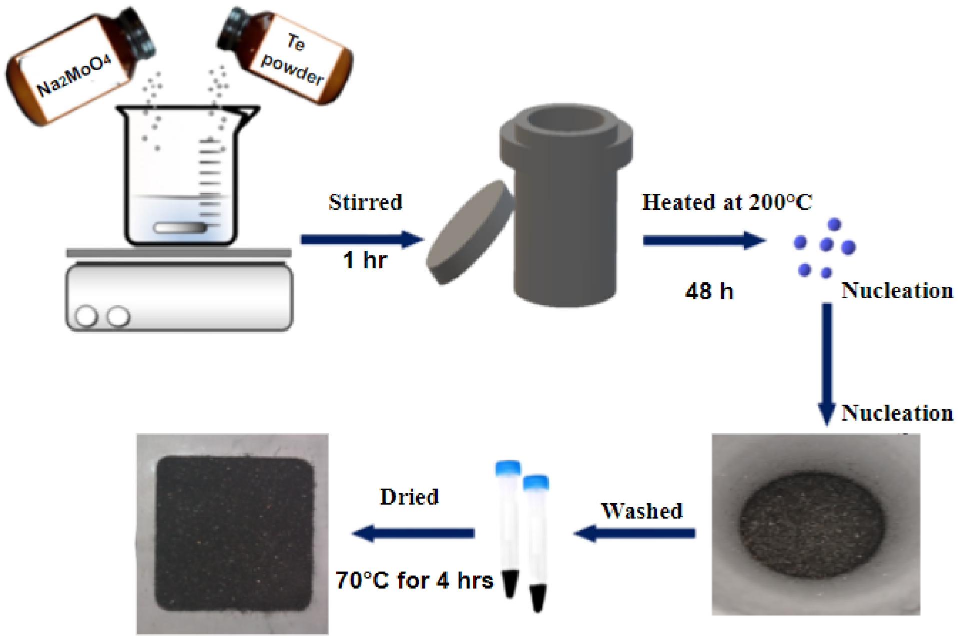

Fig.4: Synthesis of $MoTe_2$

CHAPTER-3

Characterization and measurement Techniques

3.Characterization and Measurements Techniques.

UV–Vis absorbance spectra of the synthesized samples were recorded using Shimadzu UV-2401 PC uv-vis spectrophotometer. Powder XRD pattern was obtained in the angle range of 10°–70°, using CuKα radiation (k = 1.5406 Å) with an operation voltage and current maintained at 40 kV and 50 mA. The Raman spectra were obtained using the LabRAM HR Evolution Raman system with a 532 nm laser source. The Photoluminescence spectra was recorded using the Cary Eclipse Fluorescence Spectrophotometer.

3.1. UV-VIS Spectroscopy

UV-VIS spectroscopy is a physical technique in optical spectroscopy that uses light in the visible, ultraviolet, and near-infrared ranges. It is based on Beer-Lambert law which states that the absorbance of a solution is directly proportional to the concentration of the absorbing species present in the solution and the path length. Therefore, for a fixed path length, it can be used to determine the concentration of the absorber in a solution. A molecule or ion will exhibit absorption in the visible or ultraviolet region when the incident radiation causes an electronic transition within its structure. Thus, the absorption of light by the sample is accompanied by a change in the electronic state of the molecules. The energy supplied by the light promotes the electrons from their ground state orbital to higher energy excited state orbital or antibonding orbital.

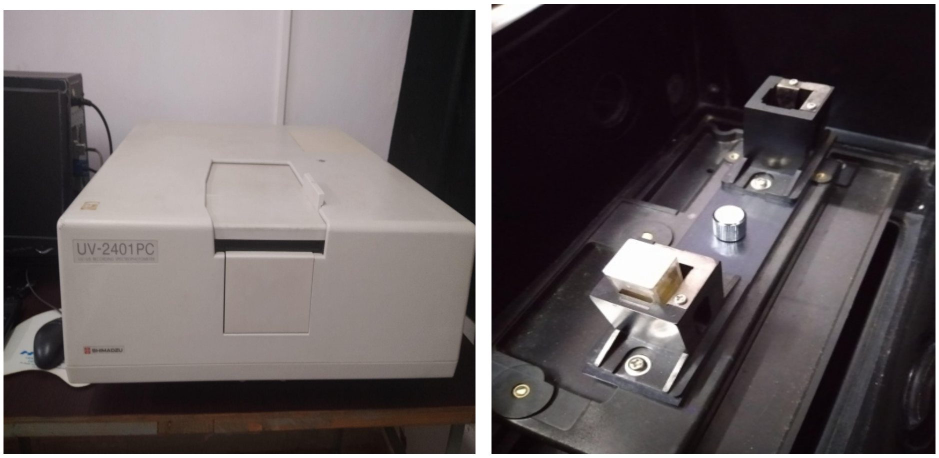

Fig.5. UV-Visible Spectrophotometer

3.2.X-ray Diffraction

X-ray diffraction (XRD) is a powerful nondestructive technique which is widely used in the characterizing crystalline materials and it provides information on structures, phases, preferred crystal orientations (texture), as well as other structural parameters, such as average grain size, crystallinity, strain, and crystal defects. X-ray diffraction peaks are produced by the constructive interference of a monochromatic beam of X-rays scattered at specific angles from each set of lattice planes in a sample. The intensity of the peaks is determined by the distribution of atoms within the lattice. Consequently, the X-ray diffraction pattern gives the fingerprint of periodic atomic arrangements in a given material.

Fig.6.Rigaku XRD machine

3.3. Raman spectroscopy

Raman spectroscopy is a very powerful tool for material analysis which allows us to explore the properties of a wide range of different materials. It has been used to investigate several features of materials such as inorganic properties, providing useful information on their phases, functions, and defects. Furthermore, techniques such as surface enhanced Raman spectroscopy (SERS) have extended the field of application of Raman analysis to biological and analytical fields. In Raman spectroscopy, the sample is illuminated with a monochromatic laser beam which interacts with the molecules of the sample and gives rise to scattered light. This scattered light has a frequency different from that of incident light (inelastic scattering) and is used to construct the Raman spectrum. When a monochromatic radiation strikes at sample, it scatters in all directions after its interaction with sample molecules and much of this scattered radiation has a frequency which is equal to frequency of incident radiation and constitutes Rayleigh scattering while a small fraction of scattered radiation has a frequency different from frequency of incident radiation which constitutes Raman scattering. When the frequency of incident radiation is more than frequency of scattered radiation, Stokes lines appear in Raman spectrum while when the frequency of incident radiation is lower compared to frequency of scattered radiation, anti-Stokes lines appear in spectrum.

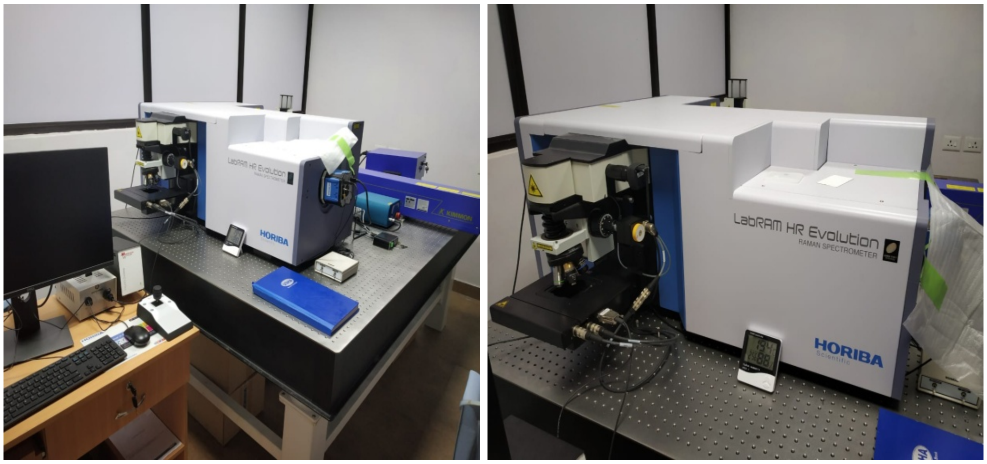

Fig. 7. Horiba Scientific LabRAM HR Evol Raman system

3.4. Scanning Electron Microscopy (SEM)

The scanning electron microscope (SEM) makes use of a focused beam of high-energy electrons to generate a variety of signals at the surface of solid specimens. These signals that derive from electron-sample interactions give the information about the sample including external morphology (texture), chemical composition, and crystalline structure and orientation of materials making up the sample. In most applications, data is collected over a selected area of the surface of the sample, and a 2-dimensional image is generated that displays spatial variations in these properties. The secondary electrons and backscattered electrons are most frequently used for imaging the samples.

Fig.8. SEM instrument-Zeiss EVO 18 system

3.5. Photoluminescence Spectroscopy

Photoluminescence spectroscopy, often referred to as PL, occurs when light energy, or photons, stimulate the emission of a photon from any matter. It is a non-contact, nondestructive method of probing materials. In particular, light is directed onto a sample, where it is absorbed and where a process called photo-excitation can occur. The photo-excitation causes the material to jump to a higher electronic state, and will then release energy (photons) as it relaxes and returns back to a lower energy level. The emission of light or luminescence through this process is photoluminescence, PL.

Photoluminescence takes on three forms: fluorescence, phosphorescence and chemiluminescence. Fluorescence is a type of luminescence caused by photons exciting a molecule, raising it to an electronic excited state. The excited state undergoes rapid thermal energy loss to the environment through vibrations, and then a photon is emitted from the lowest-lying singlet excited state. This process of photon emission competes for other non-radiative processes including energy transfer and heat loss.

Fig .9. Fluorescence Spectrophotometer

CHAPTER-4

Results and Discussion

4.Results and Discussion

4.1.UV-Vis Spectroscopy

4.1.1aUV-Vis Spectroscopy of ZnSe

The curves in Fig.9. and Fig.10. show the UV–Vis absorbance spectra of the ZnSe synthesized at EDTA=2.02g and EDTA=1.05 g respectively. Energy band gap from the Kubelka-Munk function was found to be E_g=2.77eV and E_g=2.70 eV respectively.

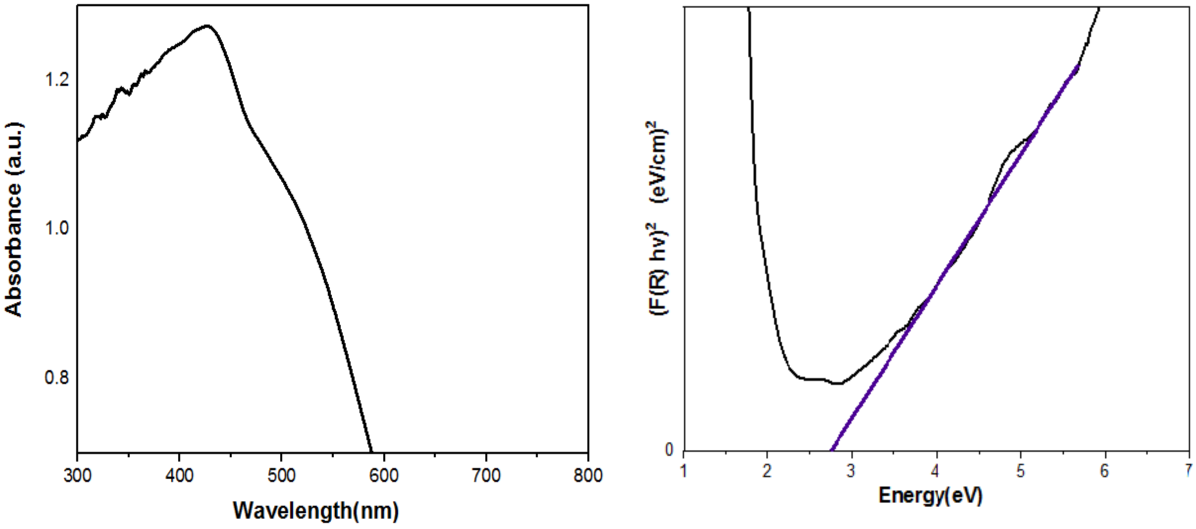

(a) **(b)**

Fig.10.(a) UV-Vis DRS spectra (b) Kubelka-Munk model of ZnSe nanostructures with EDTA=2.02g.

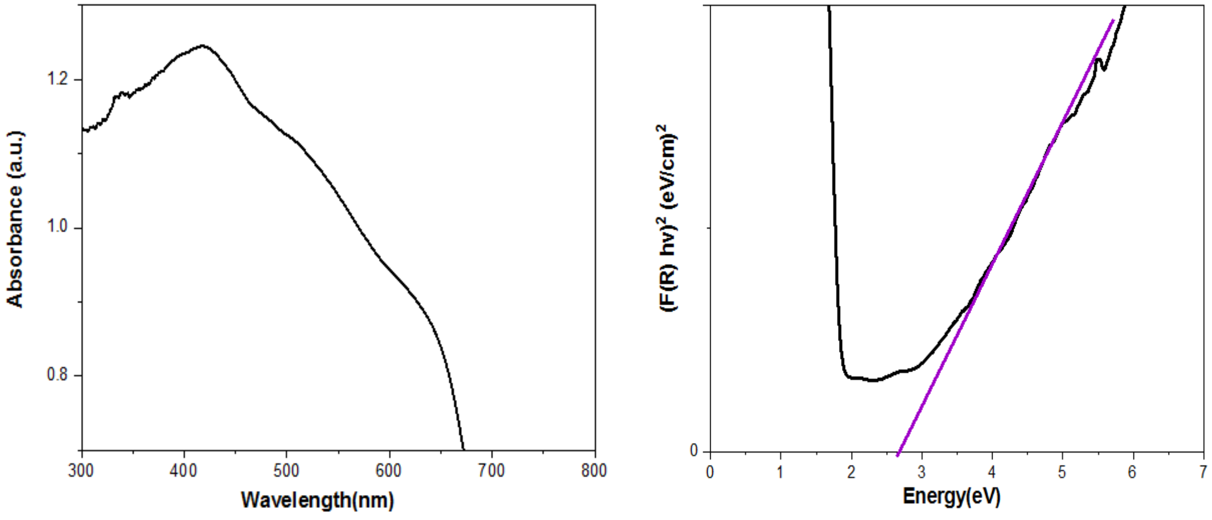

(a) **(b)**

Fig.11. (a) UV-Vis DRS spectra (b) Kubelka-Munk model of ZnSe nanostructures with EDTA=1.05g.

4.2.1b. UV-Vis Spectroscopy of MoS_2

The curves in Fig.11. show the UV–Vis DRS spectra of the synthesized sample recorded using Shimadzu UV-2401 PC UV-Vis spectrophotometer. Energy band gap from the was found to be 2.11eV for MoS_2 from Kubelka-Munk model.

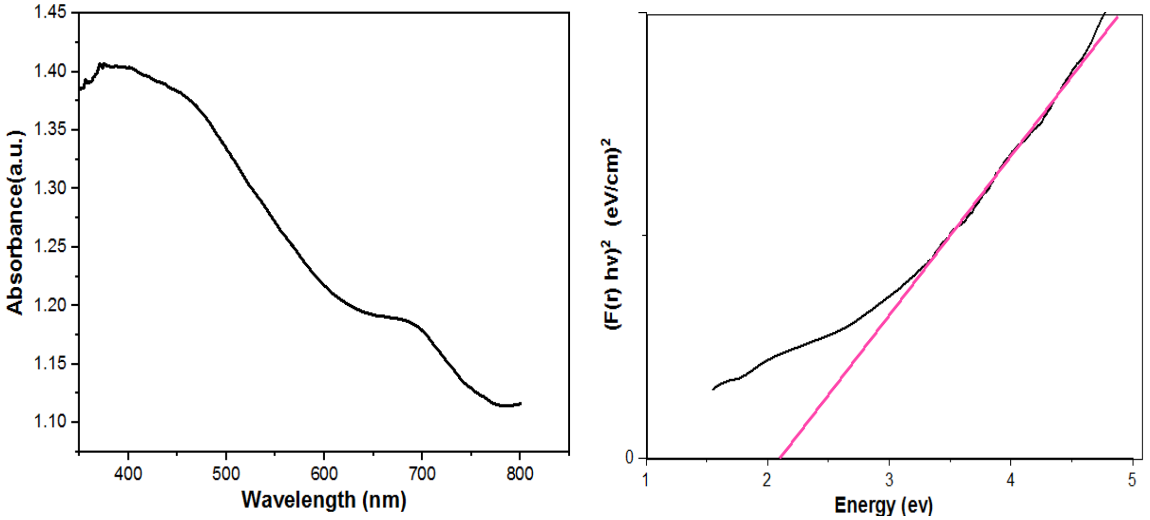

(a) (b)

Fig.12. (a) UV-Vis DRS spectra of MoS2 (b) Kubelka-Munk model. Energy band gap =2.11eV(direct band gap).

4.2.1.c. UV-Vis Spectroscopy of $MoSe_2$

The curves in Fig.12. show the UV–Vis absorbance spectra for $MoSe_2$. Energy band gap from the was found to be 1.55 eV from Tauc plot.

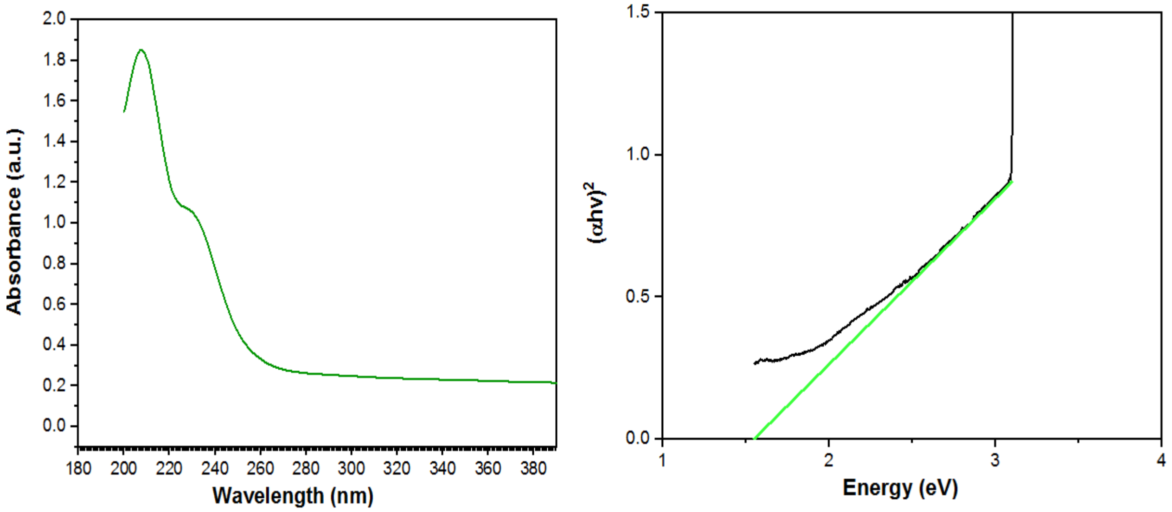

(a) (b)

Fig.13. (a)UV-Vis spectra of $MoSe_2$ (b) Energy band gap =1.55eV from Tauc plot.

4.2. X-ray Diffraction

4.2.2a. X-ray Diffraction of ZnSe

The Powder XRD pattern was obtained in the angle range of 10–70, using CuKα radiation (k = 1.5406 Å) with an operation voltage and current maintained at 40kV and 50 mA. All the diffraction peaks in the pattern can be indexed to Wurtzite (hexagonal) structure.

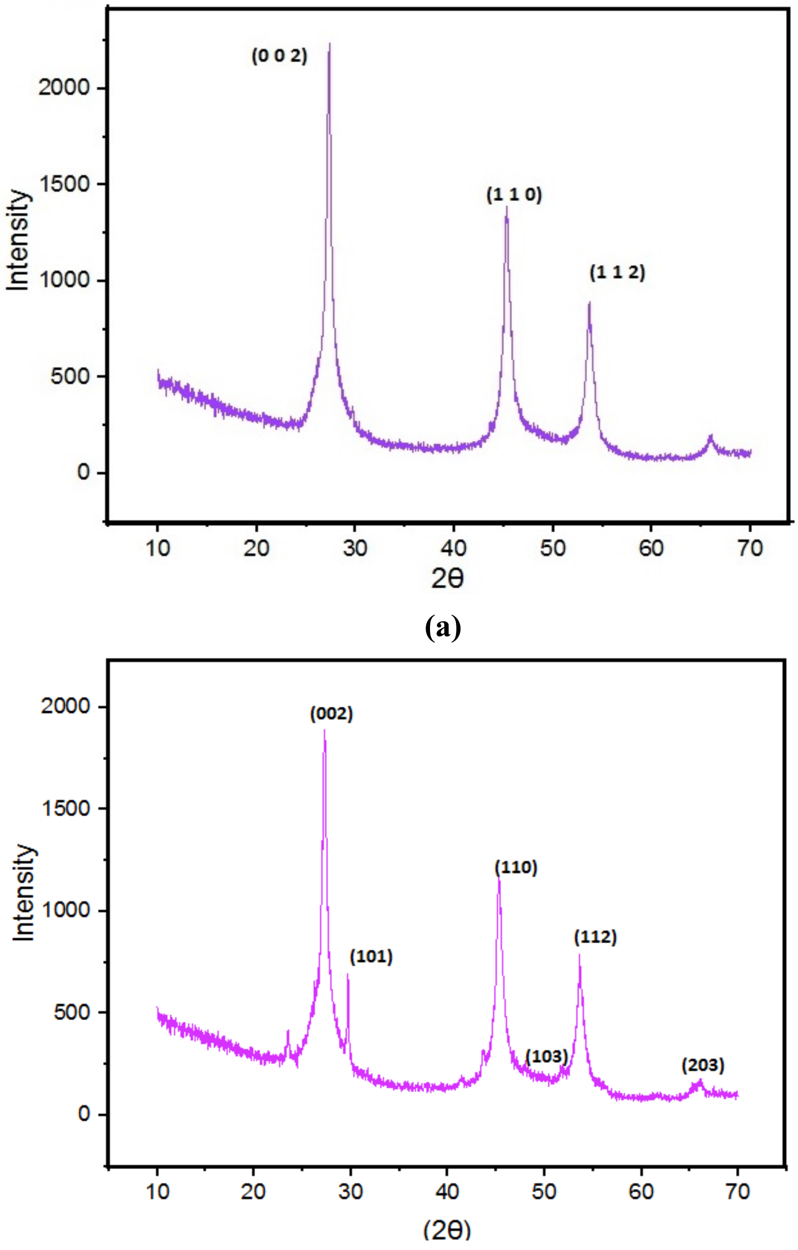

(a)

(b)

Fig.14. XRD pattern of ZnSe with hydrothermal treatment time for 2 hrs. at the hydrothermal treatment temperature of 180 °C. (a) EDTA = 2.02g (b)1.05g.

4.2.2b. X-ray Diffraction of Molybdenum Dichalcogenide (MoX_2; X=S, Se, Te) nanostructures

The XRD pattern of MoS_2 as seen in Fig.13a. exhibited two main peaks at 33.20 ° and 57.23 ° which were attributed to the (100) and (110) peaks of the 2H-MoS_2 synthesized at 200°C whereas, the XRD pattern exhibited two additional peaks at 14.2° and 39.5° corresponding to (002) and (103) peaks of 2H MoS_2 when synthesized at 210° C as seen in Fig 15b.

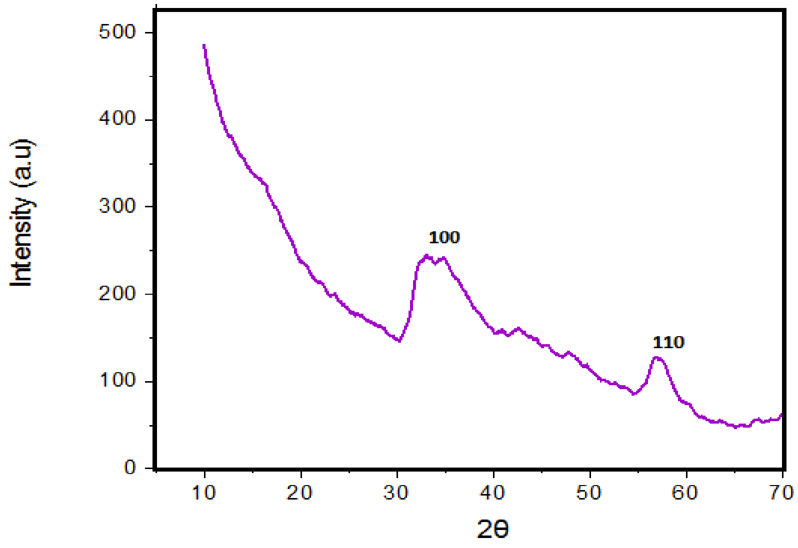

(a)

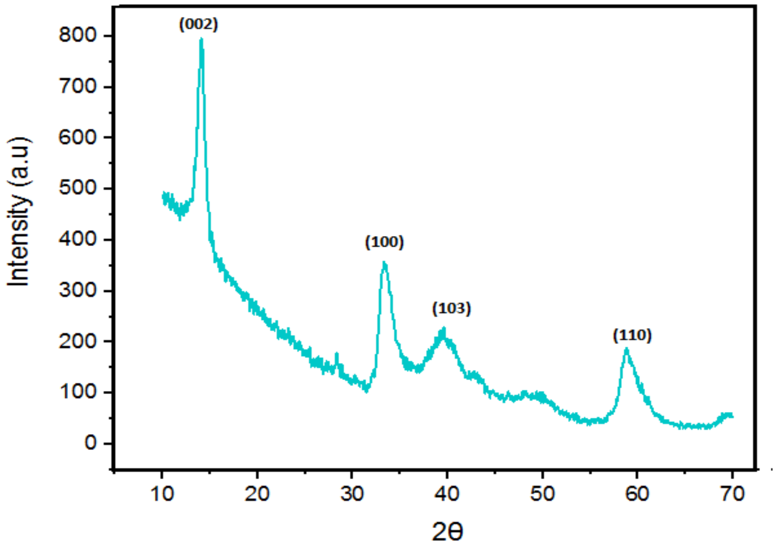

(b)

Fig.15. (a)PXRD pattern of MoS_2 synthesized at 200°C (b)PXRD pattern of MoS_2 synthesized at 210°C.

The Fig.16 displays the XRD pattern of $MoSe_2$ indexed to its hexagonal phase. The XRD pattern in Fig.17. indicates the peaks corresponding to $MoTe_2$ and weaker Te rings with the pattern indexed to their hexagonal phase.

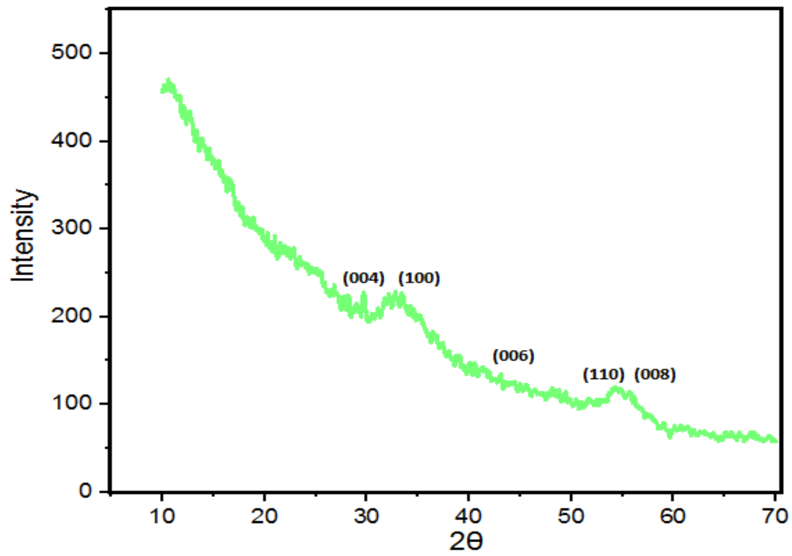

Fig.16.XRD pattern of $MoSe_{2.}$

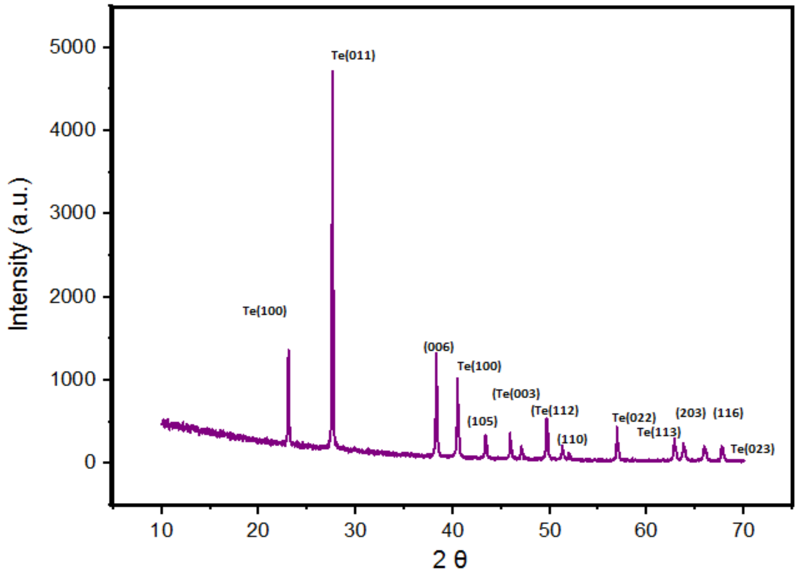

Fig.17. PXRD pattern of $MoTe_2$

4.3. Raman Spectroscopy

4.3.3a. Raman Spectra of ZnSe

Raman spectra of synthesized samples were recorded at room temperature using a 532nm laser.

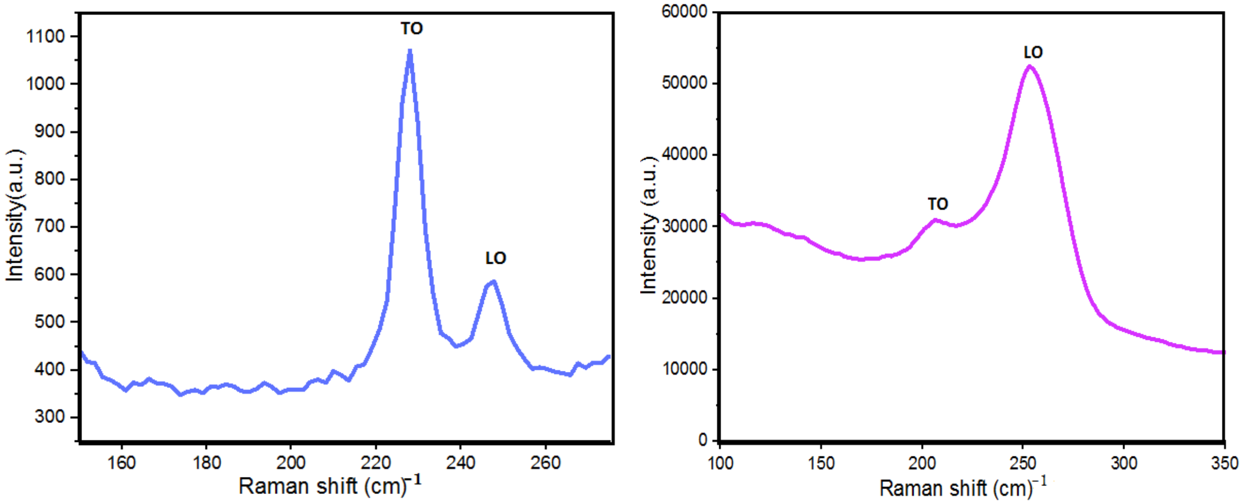

(a) **(b)**

Fig.18. Raman spectra of ZnSe with hydrothermal treatment time for 2 hrs at the hydrothermal treatment temperature of 180°C with (a) EDTA=2.02g (b)EDTA=1.05g.

4.3.3b.Raman Spectra of Molybdenum Dichalcogenide (MoX_2; X=S, Se, Te) nanostructures

The spacing between E^1_{2g} and A_{1g} modes of the monolayer, two layers, three layers, and bulk of MoS_2 is known as 18–19 cm-1,22 cm-1, 23–24 cm-1, and 25–26 cm-1, respectively [13]. In Fig.16a Raman spectra of MoS_2 depict two prominent modes E'2g which appear 380 cm-1 due to in plane vibration and A1g mode which appears 405cm-1 due to out of plane vibration mode.The appearance of two first-order Raman active modes E^1_{2g} and A_{1g} confirmed the formation of MoS_2. Fig 16b displays the Raman spectra of $MoSe_2$ with peaks at 287 cm-1 and 239 cm-1 that correspond to that of 2H $MoSe_2$. Fig 16c shows the Raman spectra of $MoTe_2$ with peak positions 264 cm^{-1},139 cm^{-1} and 121 cm^{-1}.

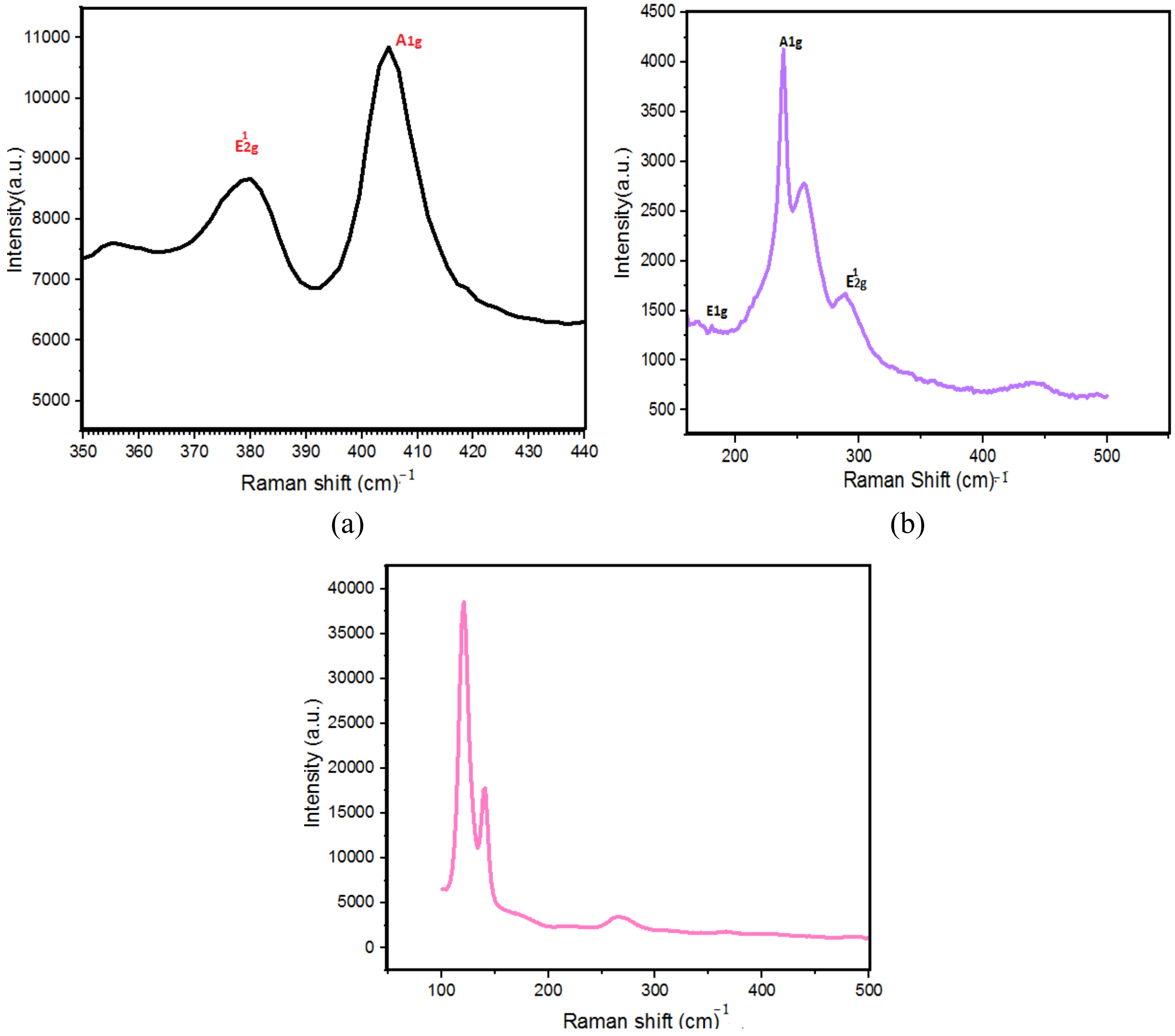

(a)

(b)

(c)

Fig.19. Raman Spectra recorded at excitation wavelength 532 nm (a) MoS_2 (b) $MoSe_2$ (c) $MoTe_2$.

4.4.Scanning Electron Microscopy (SEM) images

SEM images were taken using the Zeiss EVO 18 system. The SEM images of ZnSe synthesized with less EDTA concentration shows spherical morphology as seen in Fig.21. In the hydrothermal process, 2D sheet-like nanostructures under high pressure and temperature form 3D-flower like structures[17]. The SEM image of MoS_2 synthesized at 210°C shows a 3D-flower like structure as seen in Fig.23. while the $MoTe_2$ shows spherical morphology according to Fig.25.

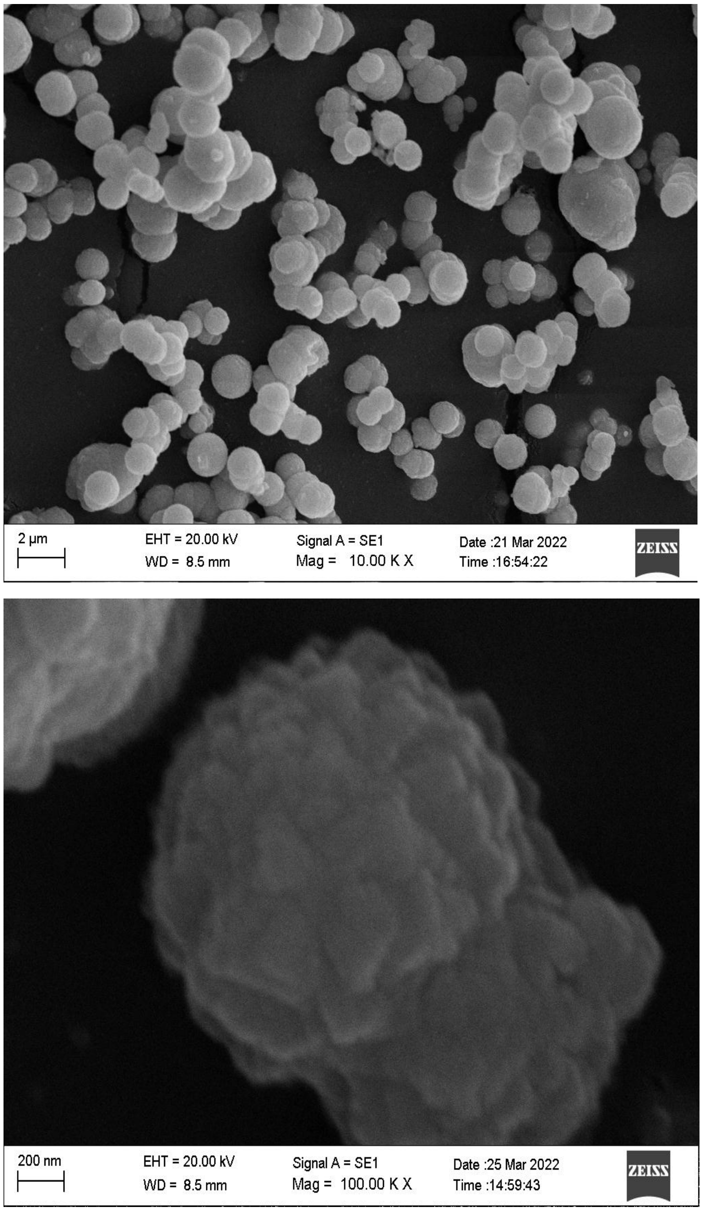

Fig.20. SEM images of ZnSe with EDTA concentration of 2.02g.

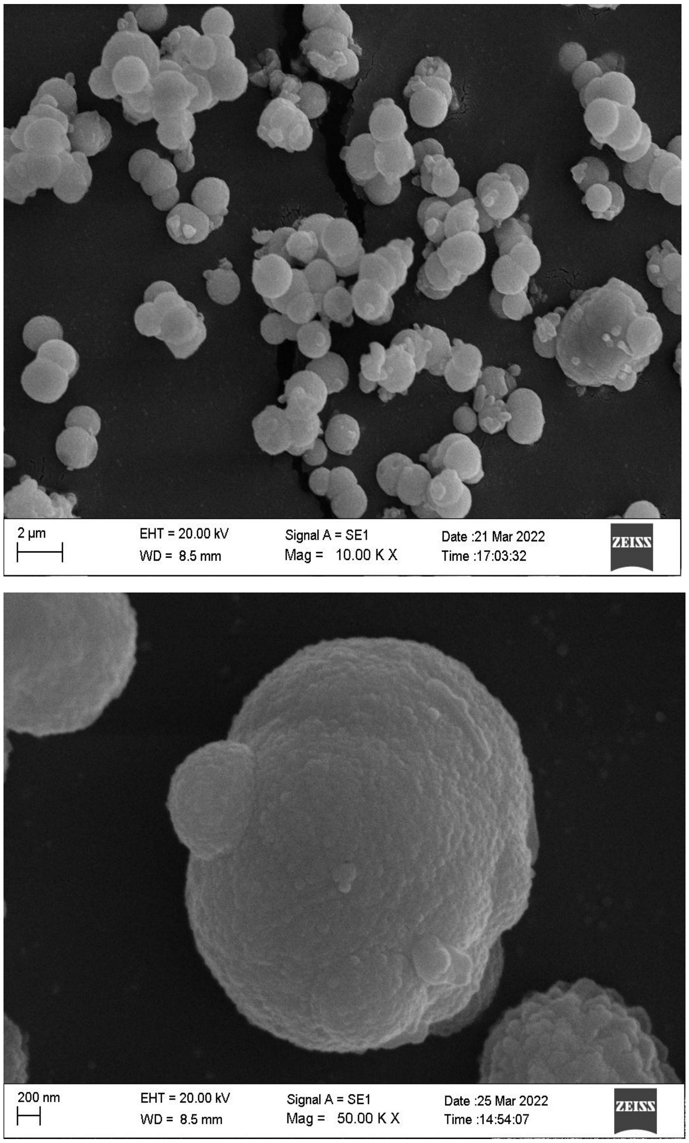

Fig.21. SEM images of ZnSe with EDTA concentration of 1.05 g.

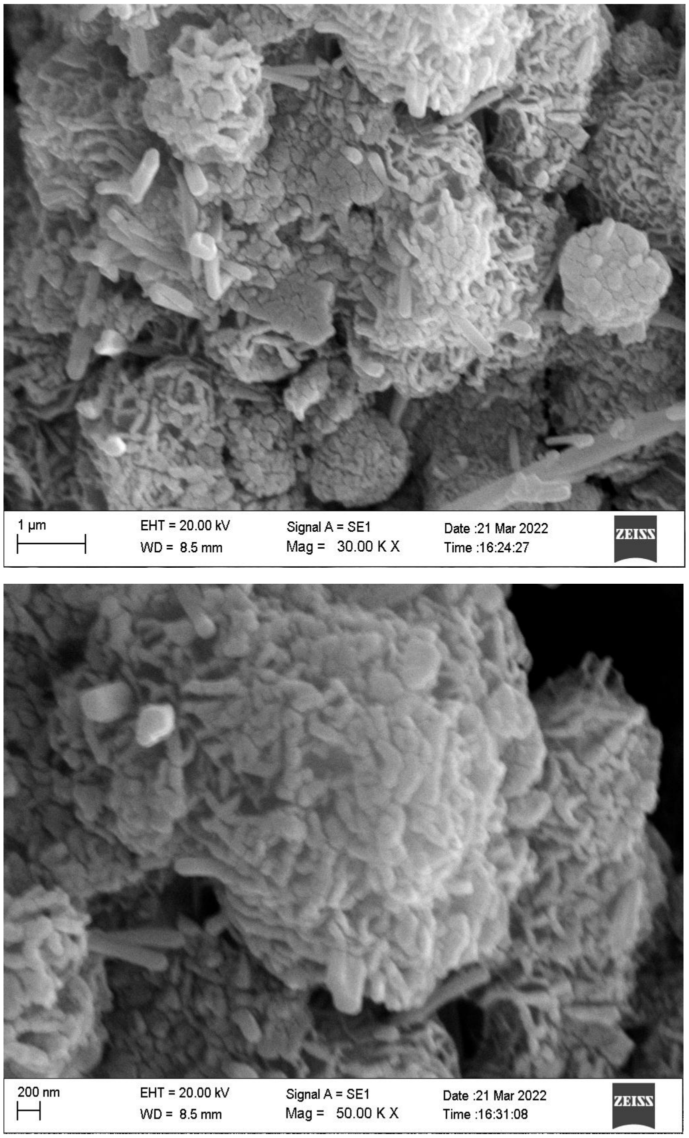

Fig.22 .SEM images of MoS_2 synthesized at 200°C

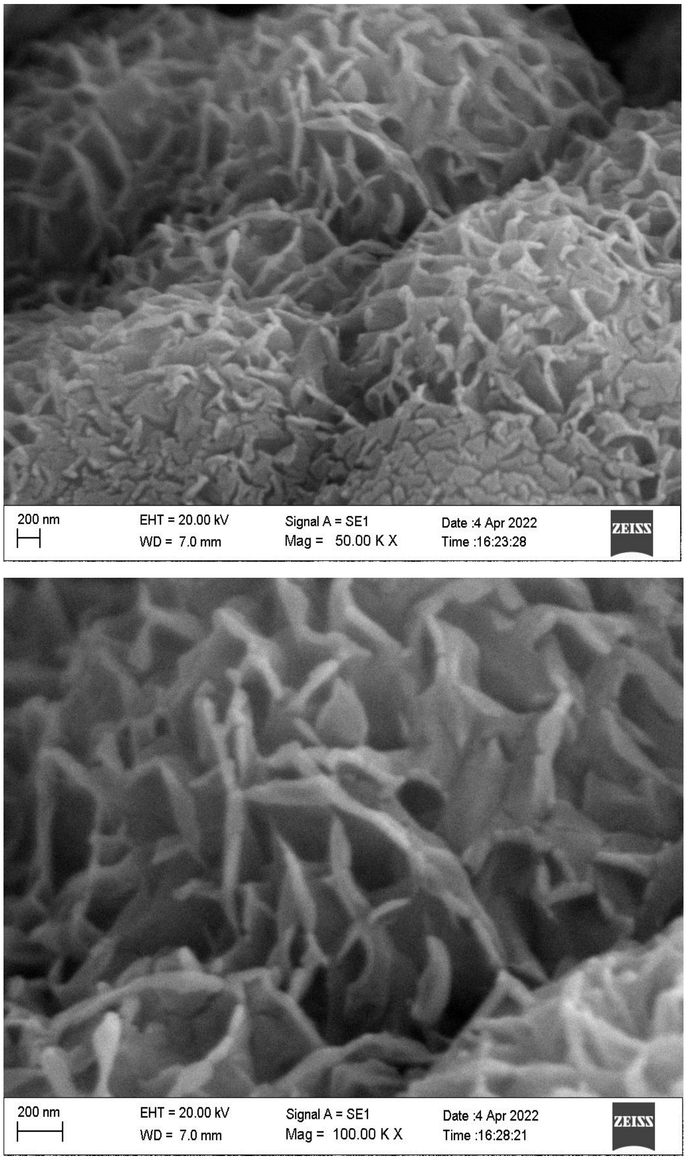

Fig.23. SEM images of MoS_2 synthesized at 210°C

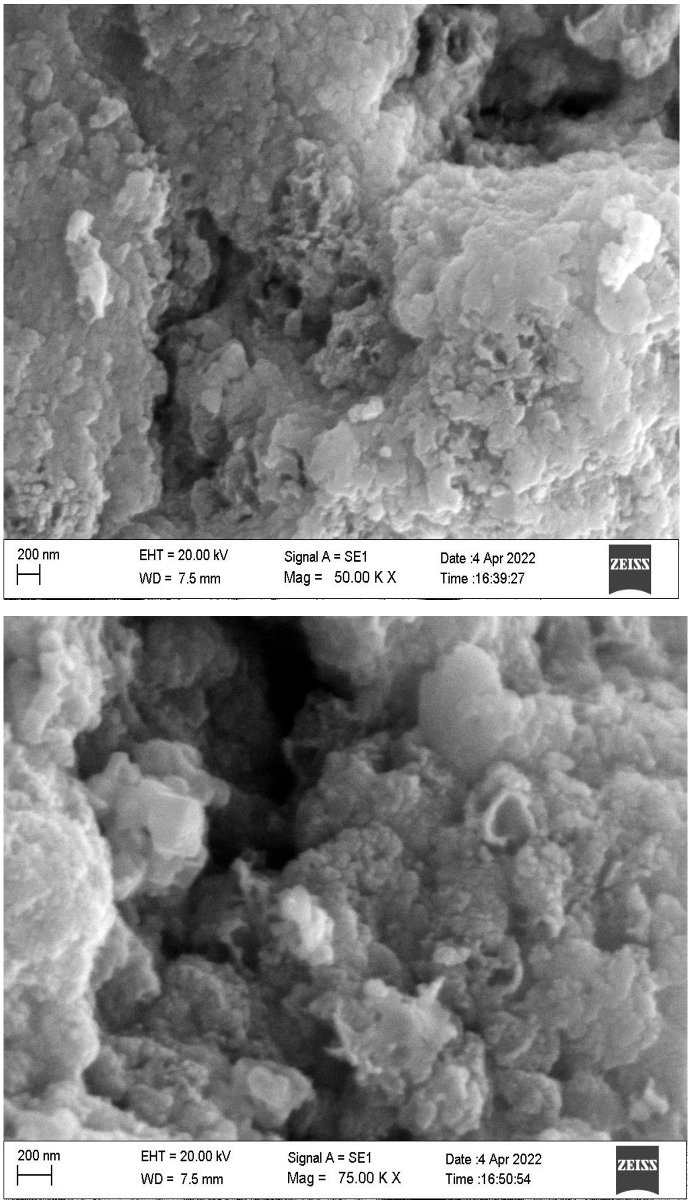

Fig.24. SEM images of $MoSe_2$ (Se=0.25g, reaction time=24 hrs)

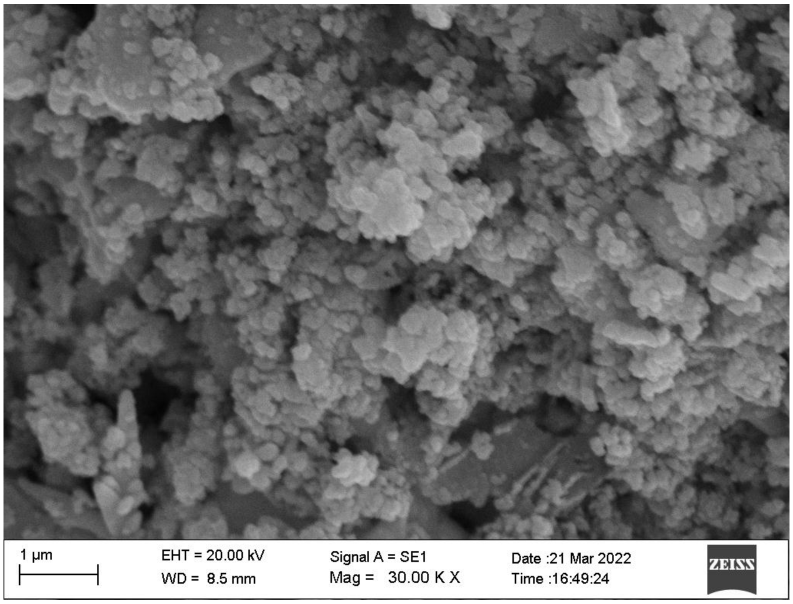

Fig.25. SEM images of $MoTe_2$ synthesized at 200°C

4.5. Photoluminescence Spectra

The Photoluminescence spectra of ZnSe was recorded at an excitation wavelength of 238 nm using the Cary Eclipse Fluorescence Spectrophotometer. The emission band at 488 nm and 554 nm are usually assigned to self-activated luminescence resulting from donor-acceptor pairs that are related to Zn vacancy and interstitial states, or associated with surface emission.

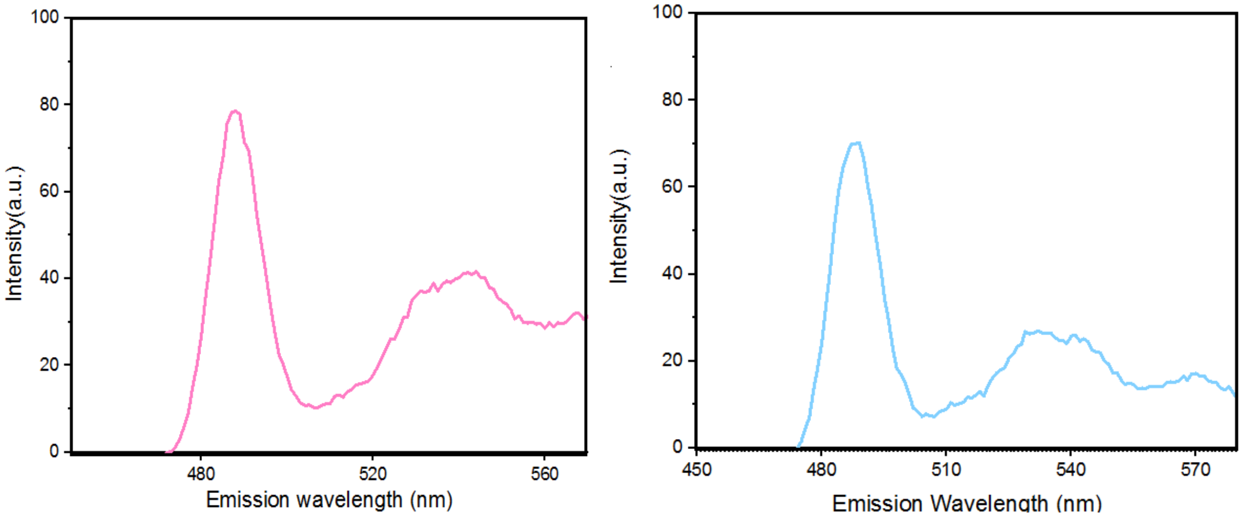

(a) **(b)**

Fig.26. Photoluminescence spectrum with(a) EDTA=2.02 g (b) EDTA=1.05g.

CHAPTER-5

Degradation of Organic Dyes

5.Degradation of organic dyes

In textile industries there are large amounts of organic mixed loaded in wastewater, which causes harmful effects and must have treated quality before reusing. Purification must be available by several different advanced techniques and many works treated on photocatalytic degradation.The most popular method however, is adsorption to remove dyes from wastewater [23].

5.1.Photocatalytic degradation

In a photocatalytic experiment the dye is brought in contact with the photocatalytic active surface of the test sample which is irradiated through the supernatant solution. The solution is decolourized in the process. Throughout the experiment the color concentration of solution is measured by UV-vis spectroscopy. For the determination of photocatalytic activity, the absorption is measured.

5.2.Photocatalytic Experiment with ZnSe

In each experiment, 2 mg of sample of ZnSe was put into a conical flask containing 60 mL RhB solution (2.5 ppm). The mixture was magnetically stirred in the dark for 1 hr 30 min. After the equilibrium was achieved the solution was illuminated with UV lamp (40 W) and after certain time intervals of UV irradiation of RhB solution, the absorption spectra were recorded using a UV-Vis Spectrometer. Complete degradation was not observed.

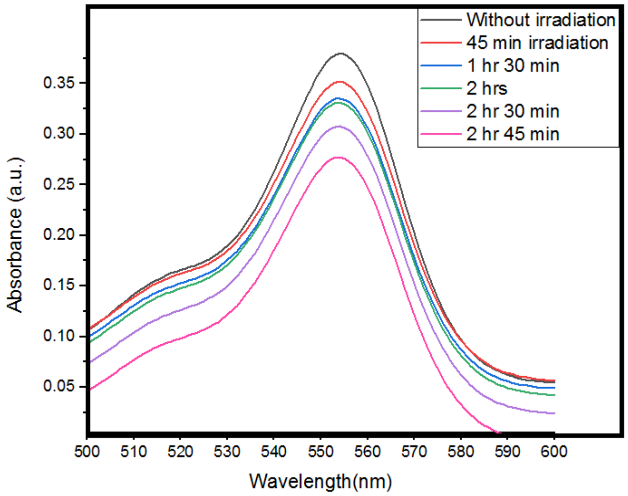

Fig.27. Photocatalytic activity of ZnSe in the degradation of rhodamine-B

5.3..Catalytic degradation of Organic dyes by adsorption

The physisorption process is regarded to be the key driving force for adsorption of the organic dyes[11]. It is a weak adsorption process in which the adsorbate is adsorbed onto the surface of adsorbent either by van der Waals or dipole-driven interaction. In this process, the chemical nature of the adsorbing pair remains intact. [16].

The adsorption kinetics and the adsorption mechanism of the dyes on the MoS2 nanosheets were investigated by linear pseudo first order (Eq. 1), linear pseudo second order (Eq. 2) and intraparticle diffusion (Eq. 3) adsorption models using UV-Vis absorption results.
The pseudo first order adsorption model is expressed by the equation:

$$\ln(Qe-Qt)=\ln(Qe - k_1 t) \text{ --------- Eq.1}$$

where Qe and Qt are the amount of dye adsorbed (mg.g-1) at equilibrium and at time t (min), respectively. k1 is the pseudo first order rate constant (min-1).
The pseudo second order adsorption model gives

$$\frac{t}{Qt} = \frac{1}{k2\,Qe^{2}} + \frac{t}{Qe} \qquad \text{---------- Eq.2}$$

where k2 is the pseudo second order adsorption process rate contact (g.mg-1.min-1)
The intraparticle diffusion model is described using following equation:

$$Q\,t= kid\; t^{0.5} + C \qquad \text{-------------Eq.3}$$

where, kid is the intraparticle diffusion rate constant (mg.g-1.min-1/2).

5.4. Surface-enhanced Raman Spectroscopy (SERS) for detection of dye concentration

SERS is a very sensitive technique which enhances the Raman scattering of molecules supported by some nanostructured materials. SERS allows structural fingerprinting of low-concentration analytes through the process of plasmon mediated amplification of electrical fields or chemical enhancement. Due to its ultra-high sensitivity and selectivity, SERS finds its application in various fields such as in surface and interface chemistry, catalysis, nanotechnology, biology, biomedicine, food science, environmental studies and other areas. Surface- enhanced Raman spectroscopy (SERS) allows for rapid, non- invasive in situ detection of target molecules.

Popular nanostructured materials used for SERS are nanoparticles (NPs), roughened films or nano- patterned substrates, enhance the Raman signals of analytes through surface plasmon enhancement or by chemical contributions. SERS relies on the use of noble metals, such as silver, gold, aluminum and copper, transition metals, or dielectric and semiconducting materials such as conductive and doped oxides. Colloidal metal NPs come in many geometric shapes beyond spheres, such as spiky silver NPs, silver nanostars, gold nanowires, silver nanoflowers, gold nanorods and gold nano snowflakes, wherein their morphologies contribute to SERS performance.

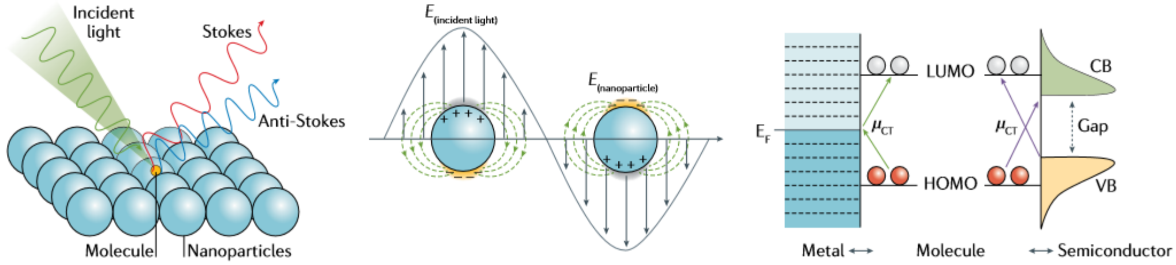

Fig.28. Mechanism of Surface-enhanced Raman scattering

Surface plasmons play a crucial role in SERS. When incident light strikes particles that are much smaller than the incident wavelength, localized surface plasmons are excited. The frequency of the induced oscillation against the restoring force between the electrons and nuclei is determined by the inherent properties of the particle, such as its size, shape and morphology. A localized surface plasmon resonance (LSPR) occurs when the light frequency matches the oscillation frequency of the electrons. This induces an enhanced electrical field near the particle surface which results in enhanced Raman scattering of adsorbates within that electromagnetic field.[19]

5.5. Catalytic Degradation of Rhodamine-B using MoS_2

The activity of the MoS_2 to degrade Rhodamine B was measured by keeping the solution in the dark while it is magnetically being stirred. In this experiment 40 mg of MoS_2 was added to a solution containing 100 mL of 5 ppm Rhodamine-B solution. The Concentration of the solution was determined using UV-Visible spectrophotometer.

Fig.29.Catalytic degradation of RhB.

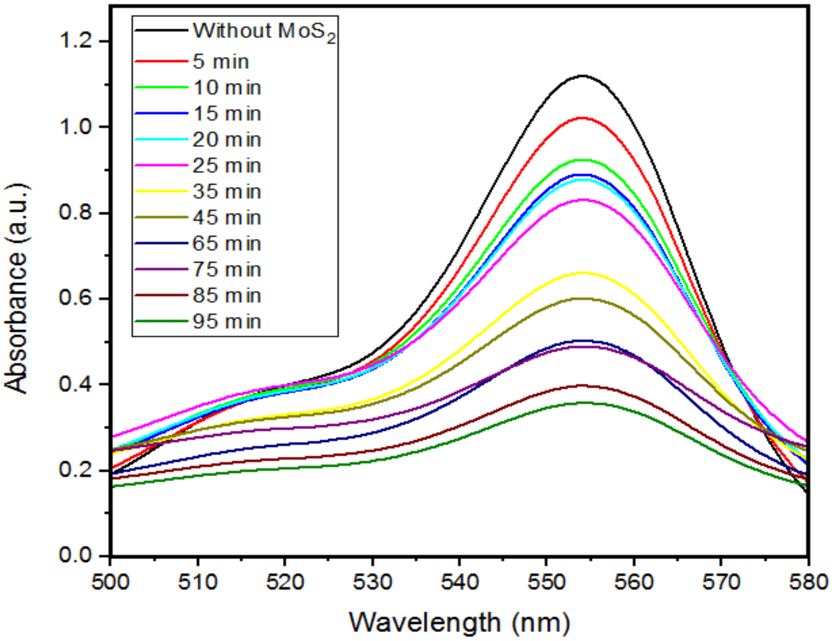

(a)

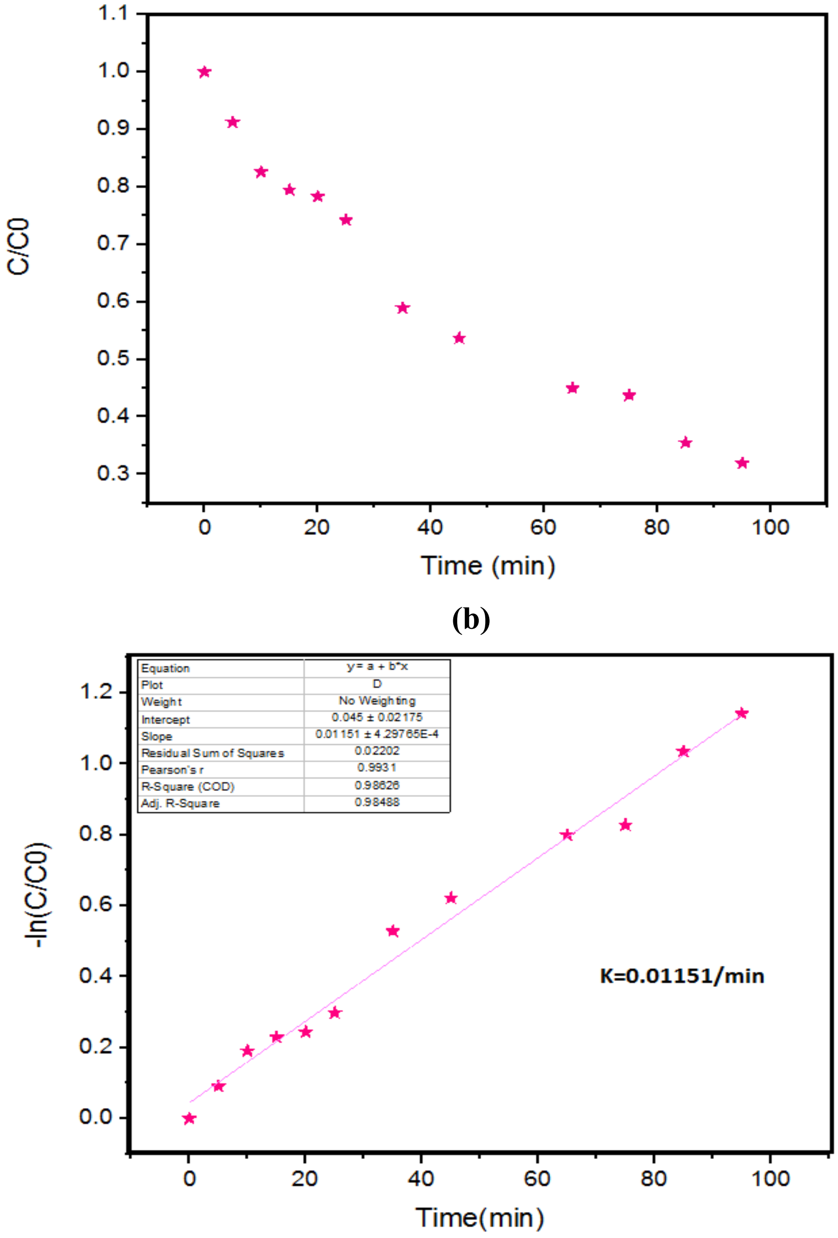

Equation	y= a + b*x
Plot	D
Weight	No Weighting
Intercept	0.045 ± 0.02175
Slope	0.01151 ± 4.29765E-4
Residual Sum of Squares	0.02202
Pearson's r	0.9931
R-Square (COD)	0.98626
Adj. R-Square	0.98488

(b)

(c)

Fig.30.(a) Absorption Spectra (b) Plot of C/Co vs t (c) Plot of -ln(C/Co) vs t

Fig.30.(c) represents a pseudo first order kinetic model. The R ^{2} values of the is found to be 0.9862 revealed that adsorption process fitted well to the pseudo first order adsorption kinetic model.

SERS Application in the detection of Rhodamine-B

Sample preparation and SERS measurements.

The most common method for performing SERS measurements is by depositing a liquid sample onto a silicon or glass surface with a nanostructured noble metal surface.

100 uL of gold-nanoparticle solution (10^{-10} M) was mixed with 100 uL of Rhodamine-B solutions collected at different time intervals after addition of MoS2. The mixture was then sonicated for 20 min and drop-casted on a silicon substrate. All samples were analyzed using a LabRAM HR Evol Raman system using a 785 nm laser source. The Raman spectra were collected between 600 and 2000 cm-1.

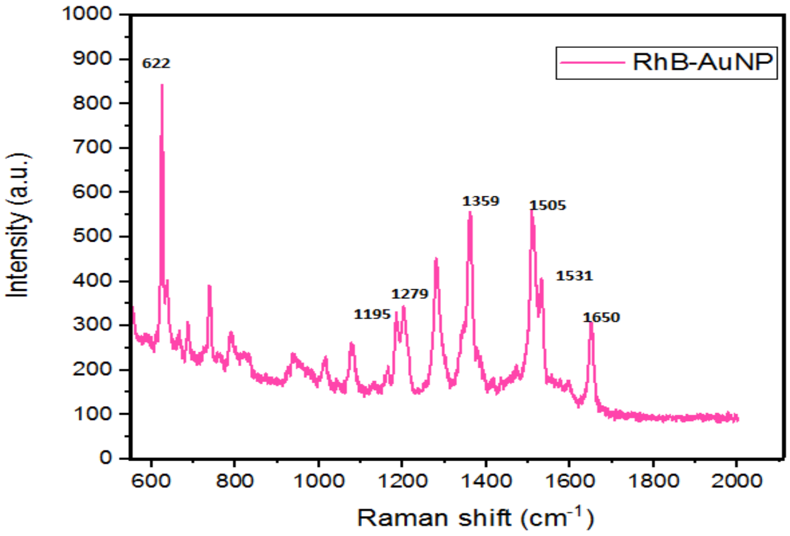

(a)

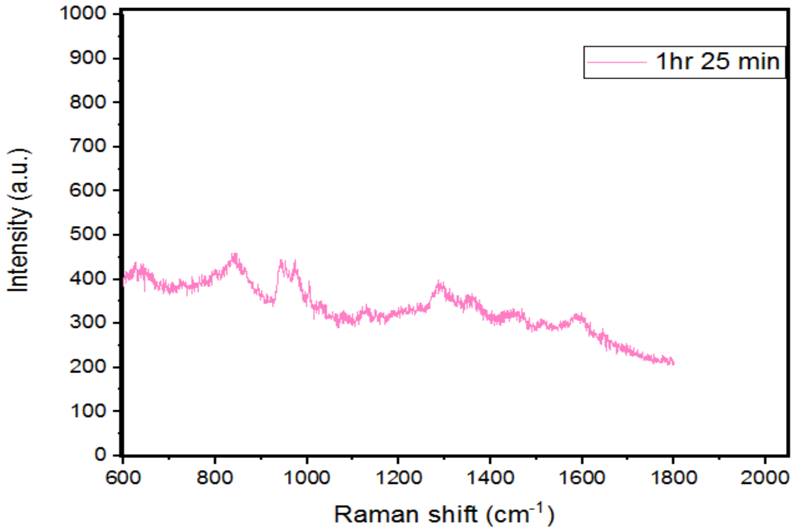

(b)

Fig.31. Raman Spectra: (a)RhB-Au (b)MoS2+RhB-Au after 1 hr 25 min.

5.6. Catalytic Degradation of Rhodamine-6G using MoS_2

The activity of the MoS_2 to degrade Rhodamine 6G was measured by keeping the solution in the dark while it is magnetically being stirred. In this experiment 40 mg of MoS_2 was added to a solution containing 100 mL of 10 ppm Rhodamine-6G solution. The solution was kept in the dark and the concentration of the solution was determined using UV-Visible spectrophotometer.

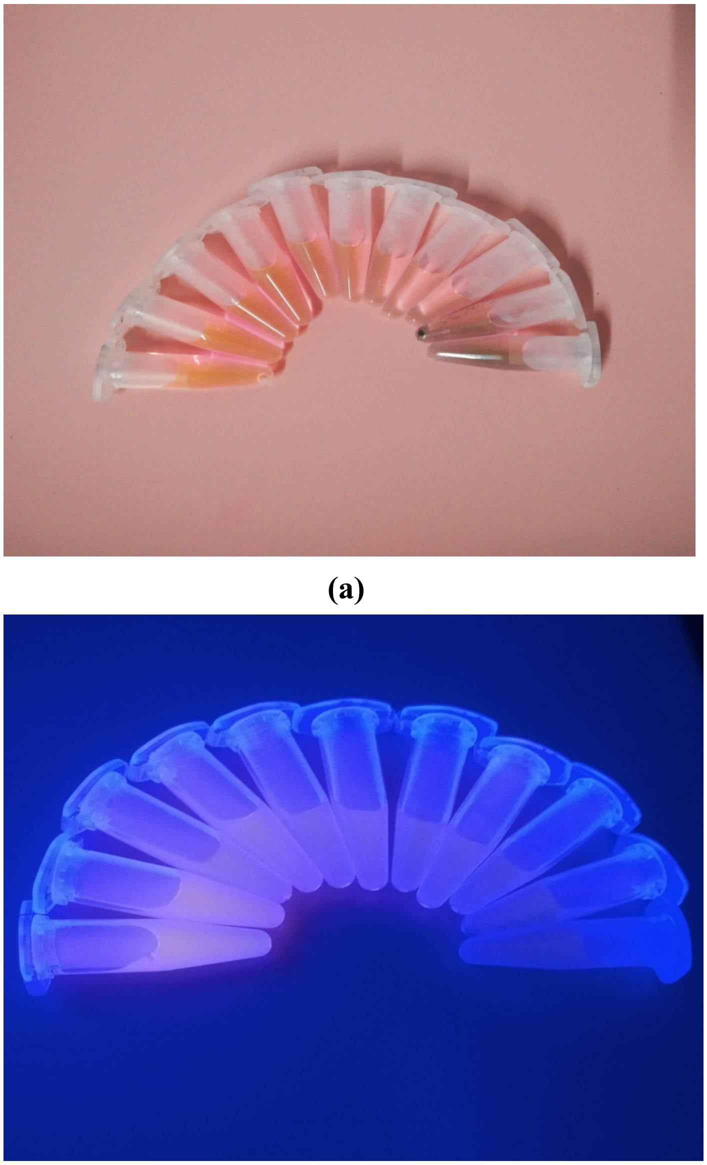
(a)

(b)

Fig .32. (a)Catalytic Degradation of Rhodamine-6G using MoS_2 (b) Photographed in UV light

Fig .33. Catalytic Degradation of Rhodamine-6G using MoS_2

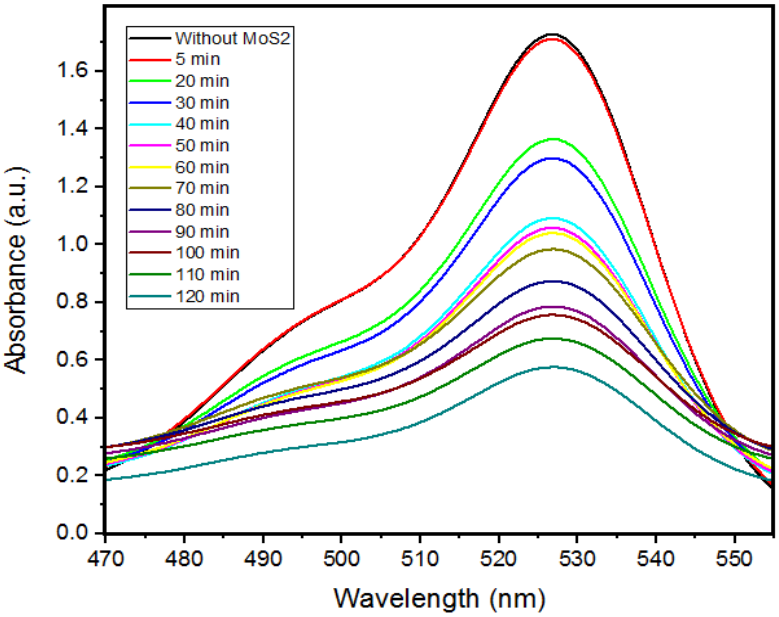

(a)

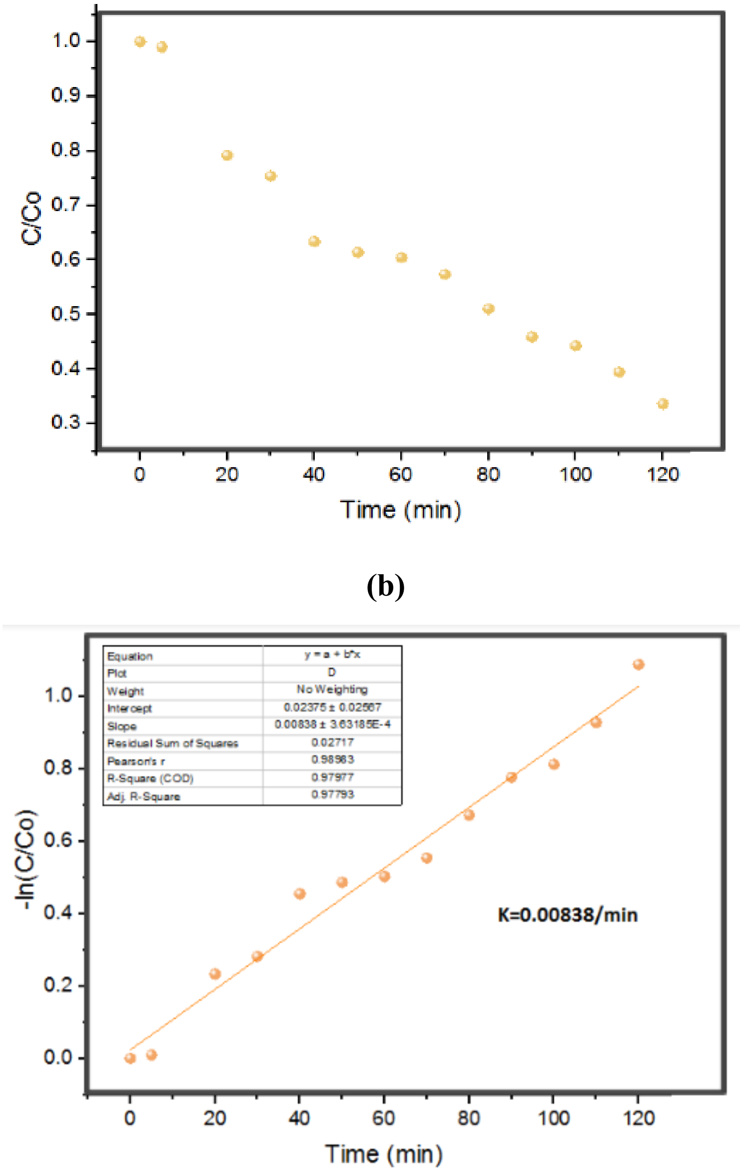

Equation	y = a + b*x
Plot	D
Weight	No Weighting
Intercept	0.02375 ± 0.02567
Slope	0.00838 ± 3.63185E-4
Residual Sum of Squares	0.02717
Pearson's r	0.98983
R-Square (COD)	0.97977
Adj. R-Square	0.97793

(b)

(c)

Fig.34. (a) Absorption spectra (b) Plot of C/Co vs t (c) Plot of -ln(C/Co) vs t

Fig.34. (c) represents a pseudo first order kinetic model. The R ^{2} values of the is found to be 0.9898 revealed that adsorption process fitted well to the pseudo first order adsorption kinetic model.

SERS Application in the detection of Rhodamine-6G

Sample preparation and SERS measurements.

100 uL of Gold-nanoparticle solution (10^{-10} M) was mixed with 100 uL of Rhodamine-6G solutions collected at different time intervals after addition of MoS_2. The mixture was then sonicated for 20 min and drop-casted on silicon wafers. All samples were analyzed using a LabRAM HR Evolution Raman system with a 785 nm laser source. The Raman spectra were collected between 600 and 2000 cm-1.

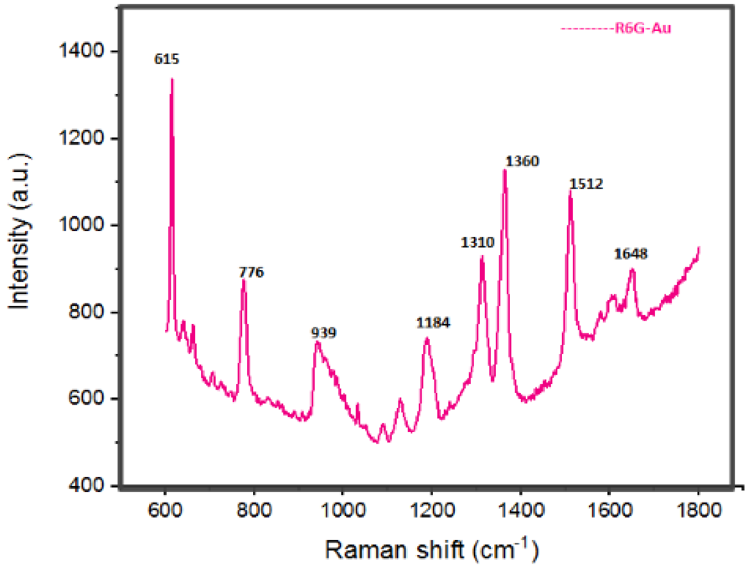

(a)

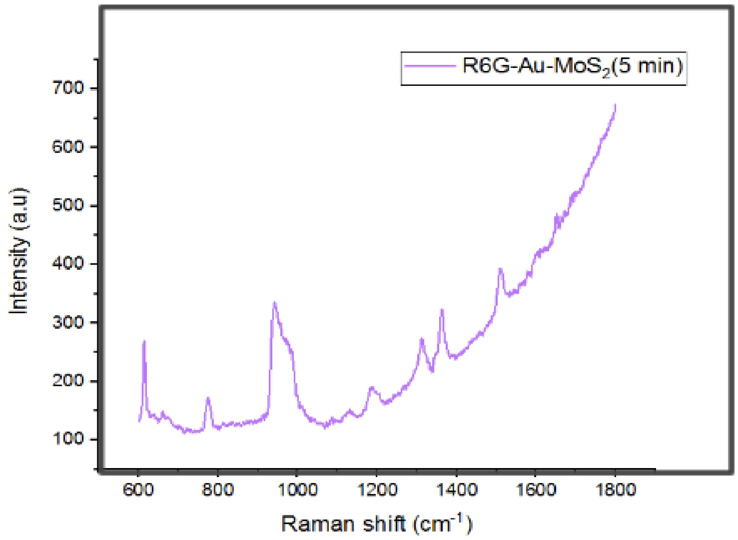

(b)

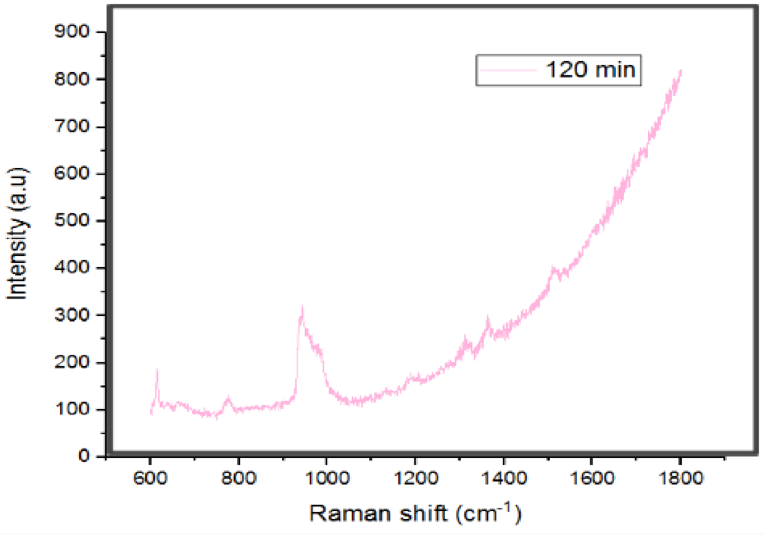

(c)

Fig.35.Raman Spectra(a)Au-R6G (b)Au-R66 5 min after adding MoS_2 (c)120 min.

Further,

(a)The activity of MoS_2 to degrade Rhodamine 6G was also measured by adding 4 mg of MoS_2 to a solution containing 5 mL of 10 ppm Rhodamine-6G solution. The concentration of the solution was determined using the UV-Visible spectrophotometer.

(b)Similar experiment was done with $MoSe_2$.

(c)Concentration of AuNP solution was changed to 2 mL.

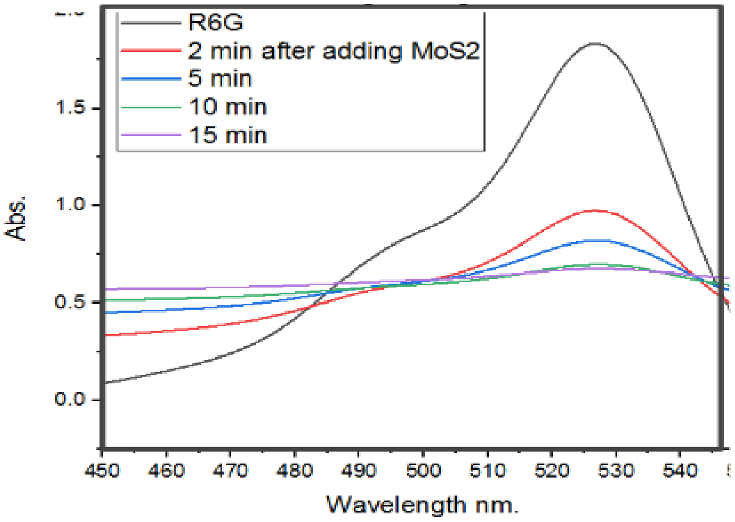

(a)

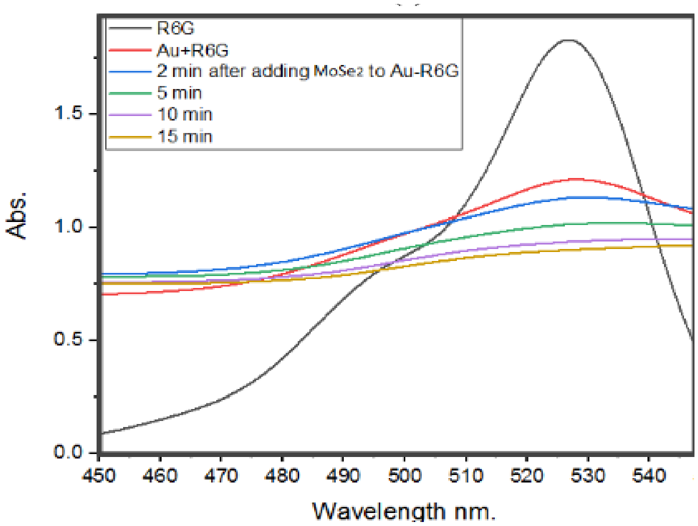

(b)

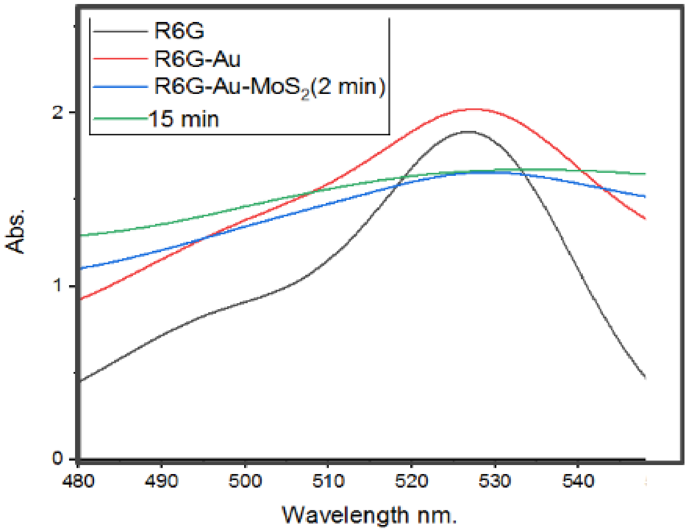

(c)

Fig.36. Absorption Spectra of degradation of R6G along with AuNP solution

5.7. Degradation of Methylene blue using MoS_2

The activity of the MoS_2 to degrade Methylene Blue was measured by keeping the solution in the dark while it is magnetically being stirred. In this experiment 15 mg of MoS_2 was added to a 10 ppm dye solution. The solution was kept in the dark and the concentration of the solution was determined using UV-Visible spectrophotometer upto 75 min of adding the sample. When the concentration of MoS_2 nanosheets was increased to 40 mg, degradation time reduced to 15 min.

Fig.37. Catalytic degradation of methylene blue

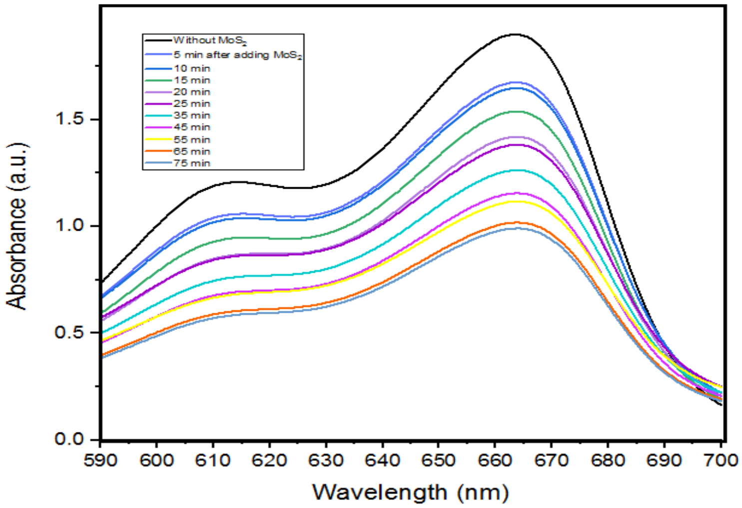

(a)

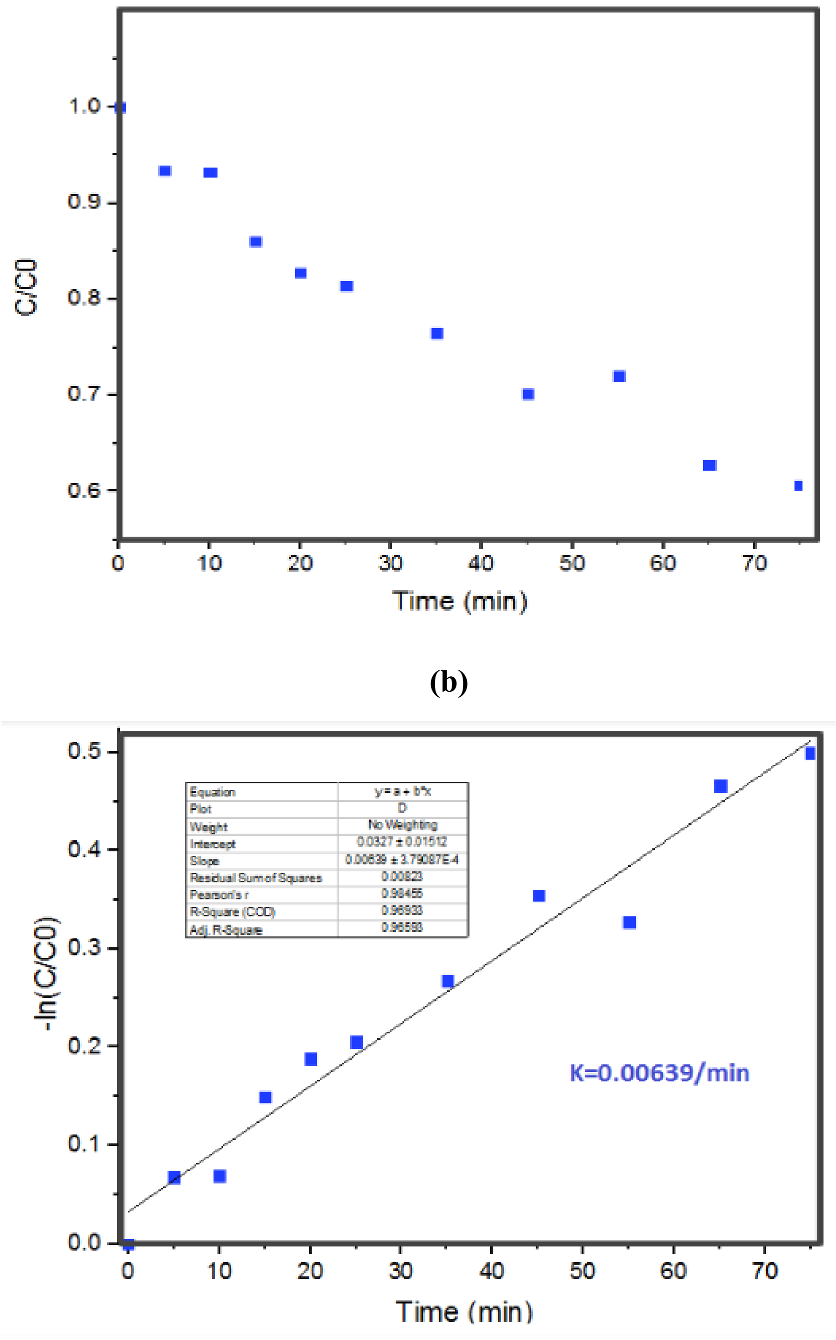

(b)

(c)

Fig.38.(a) Absorption spectra (b) Plot of C/Co vs t (c) Plot of -ln(C/Co) vs t

Fig.38c.(c) represents a pseudo first order kinetic model. The R ^{2} values of the is found to be 0.9693 revealed that adsorption process fitted the pseudo first order adsorption kinetic model.

SERS Application in the detection of Methylene Blue

Sample preparation and SERS measurements.

100 uL of Gold-nanoparticle solution(10 $^{-10}$ M) was mixed with 100 uL of Methylene blue solutions collected at different time intervals after addition of $MoSe_2$. The mixture was then sonicated for 20 min and drop-casted on silicon wafers. All samples were analyzed using a LabRAM HR Evol Raman system with a 532 nm laser source. The Raman spectra were collected between 1000 and 2000 cm-1.

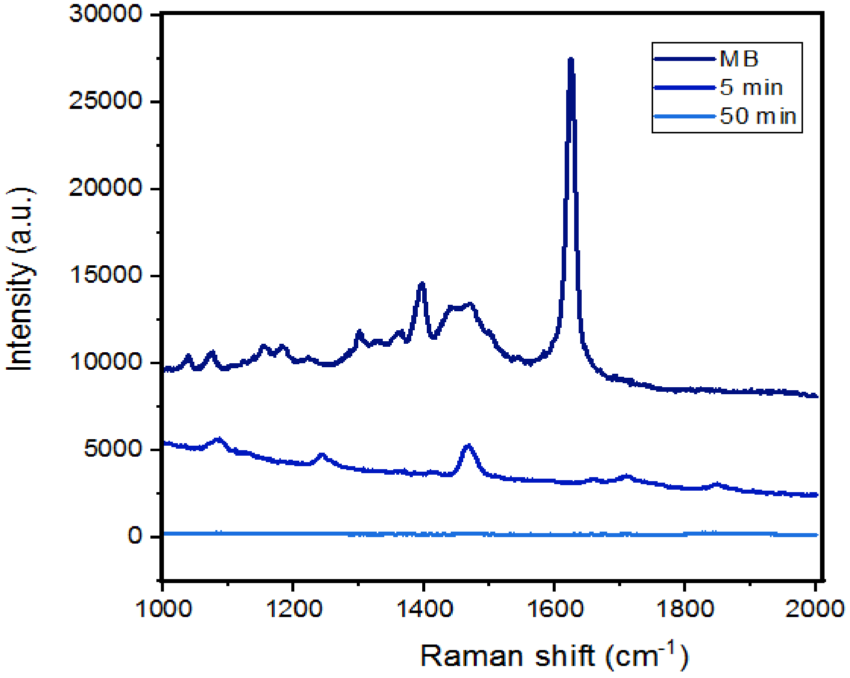

Fig.39. Raman Spectra: degradation of methylene blue

Recyclability test

The recyclability of the MoS_2 to degrade Methylene Blue was measured by adding 10 mg of MoS_2 to 3 mL of 10 ppm dye solution. The concentration of the solution was determined using the UV-Visible spectrophotometer.

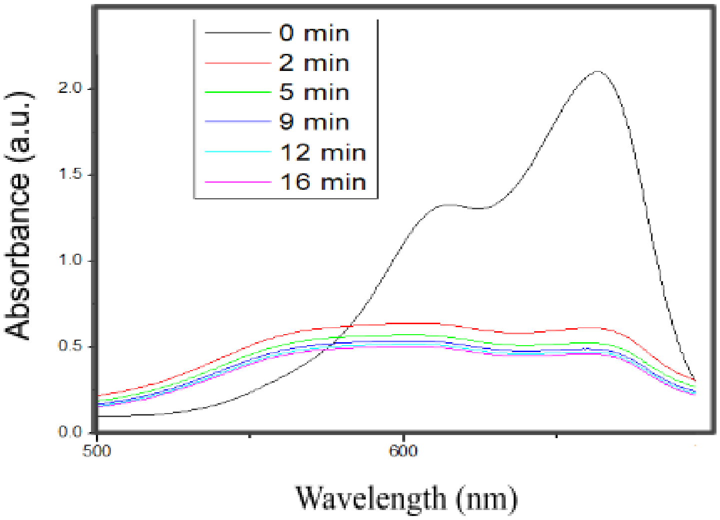

(a)

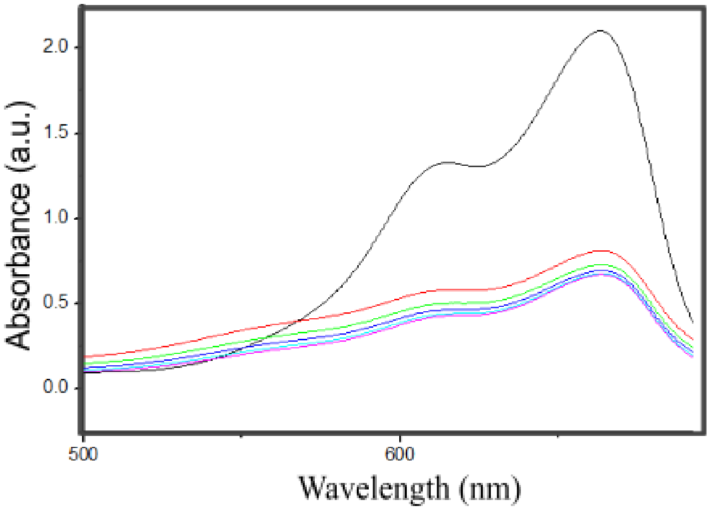

(b)

Fig.40. Recyclability test of MoS_2 (a)Catalytic degradation of MB (b) Catalytic degradation of recycled MoS_2.

5.8. Catalytic Degradation of Malachite Green using MoS_2

The activity of the MoS_2 to degrade a mixture of Malachite green was measured by keeping the solution in the dark while it is magnetically being stirred. In this experiment 40 mg of MoS_2 was added to a solution containing 20 ppm dye solution.The solution was kept in the dark and the concentration of the solution was determined using UV-Visible spectrophotometer.

Fig.41. Degradation of malachite green

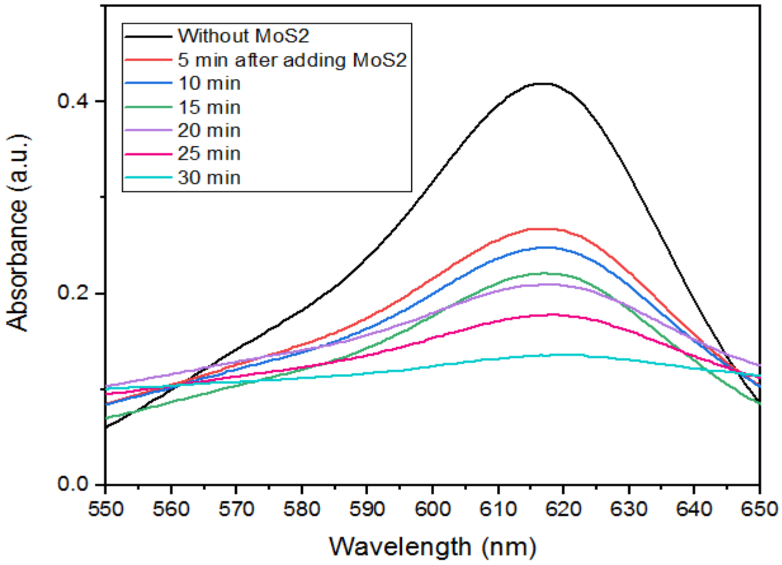

(a)

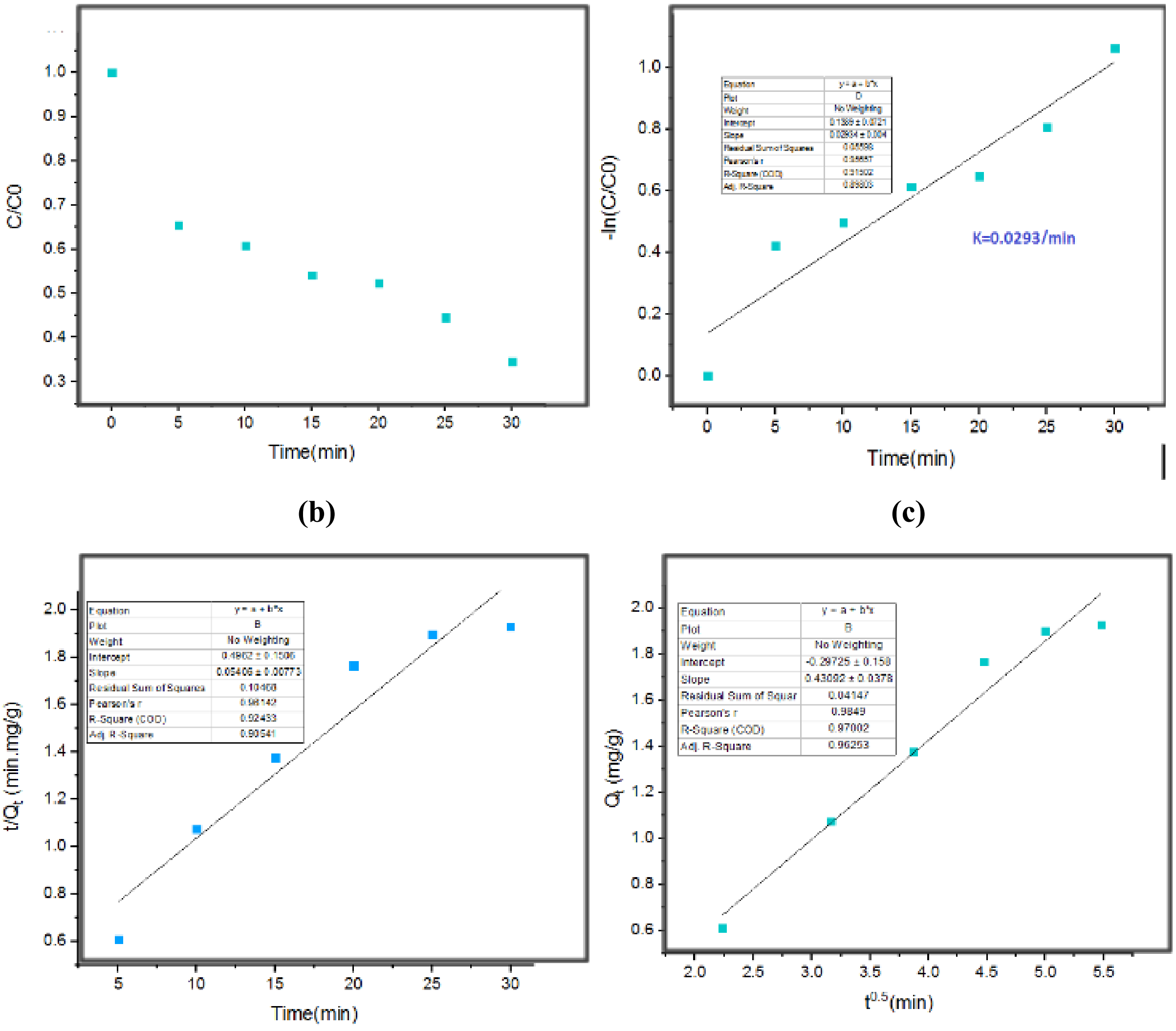

Equation	y = a + b*x
Plot	D
Weight	No Weighting
Intercept	0.1389 ± 0.0721
Slope	0.02934 ± 0.004
Residual Sum of Squares	0.05598
Pearson's r	0.95657
R-Square (COD)	0.91502
Adj. R-Square	0.89803

Equation	y = a + b*x
Plot	B
Weight	No Weighting
Intercept	0.4862 ± 0.1506
Slope	0.05406 ± 0.00773
Residual Sum of Squares	0.10468
Pearson's r	0.96142
R-Square (COD)	0.92433
Adj. R-Square	0.90541

Equation	y = a + b*x
Plot	B
Weight	No Weighting
Intercept	-0.29725 ± 0.158
Slope	0.43092 ± 0.0378
Residual Sum of Squar	0.04147
Pearson's r	0.9849
R-Square (COD)	0.97002
Adj. R-Square	0.96253

(b) **(c)**

(d) **(e)**

Fig.42.(a) Absorption Spectra (b) Plot of C/Co vs t (c) pseudo first order, (d) pseudo second order and (e) intraparticle diffusion adsorption models.

Fig.42.c represents a pseudo first order kinetic model. The R ² values of the plot are found to be 0.9150. The low values of R ² revealed that the adsorption process may not be well fitted to the pseudo first order adsorption kinetic model.

The fit of t/Qt vs. t with R ² of 0.9243 shows that the adsorption process may not be well fitted to the pseudo second order adsorption kinetic model.

The intraparticle diffusion plots (Qt vs. t $^{0.5}$) give comparatively better agreement to the linear fitting (R^2=0.9700).

SERS Application in the detection of Malachite Green

Sample preparation and SERS measurements.

100 uL of Gold-nanoparticle solution(10^{-10} M) was mixed with 100 uL of Malachite Green solutions collected at different time intervals after addition of MoS_2. The mixture was then sonicated for 20 min and drop casted on silicon wafers.All samples were analyzed using a LabRAM HR Evol Raman system with a 532 nm laser source. The Raman spectra were collected between 600 and 2000 cm-1.

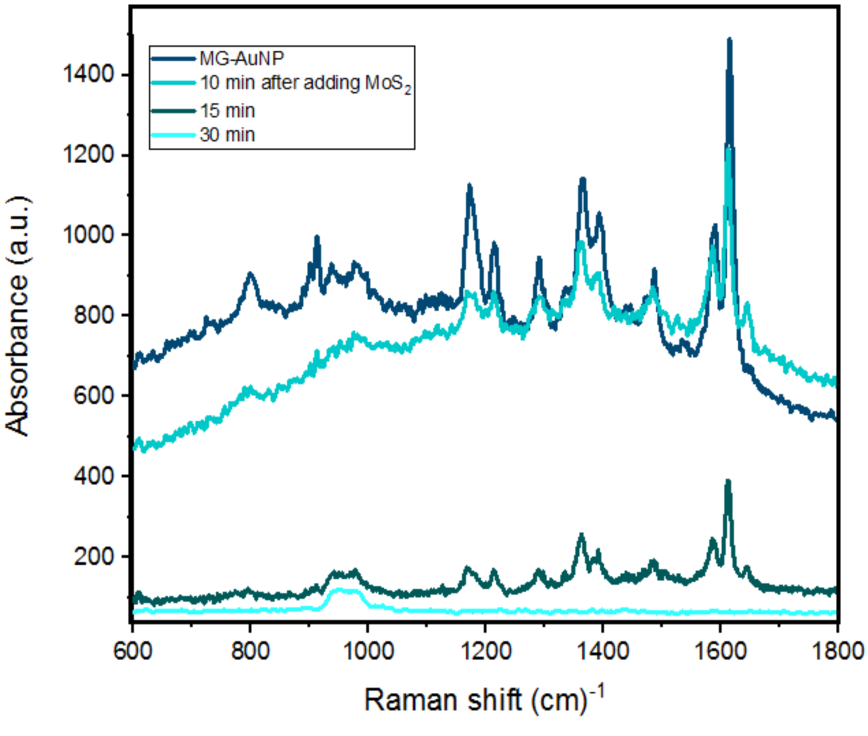

Fig.43. Raman Spectra: degradation of methylene blue

5.9.Catalytic Degradation of Methyl Orange using Molybdenum dichalcogenide(MoX_2 X=S,Se,Te) nanostructures.

The activity of Molybdenum dichalcogenide(MoX_2 ;X=S,Se,Te) nanostructures to degrade Methyl Orange were measured by keeping the solution in the dark while it is magnetically being stirred. In this experiment 40 mg of the sample was added to 10 ppm dye solution. The solution was kept in the dark and the concentration of the solution was determined using UV-Visible spectrophotometer.

(a)

(b)

Fig.44:(a)Catalytic degradation with MoS_2 (b) Catalytic degradation with $MoSe_2$

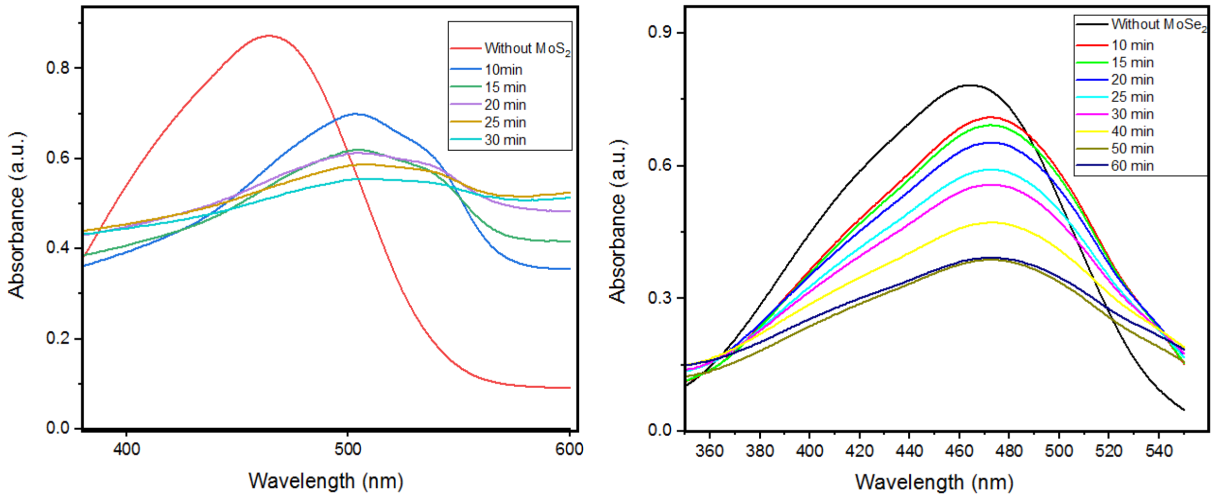

(a) **(b)**

Fig.45:Absorption Spectra (a)Catalytic degradation with MoS$_2$ (b)Catalytic degradation with MoSe$_2$

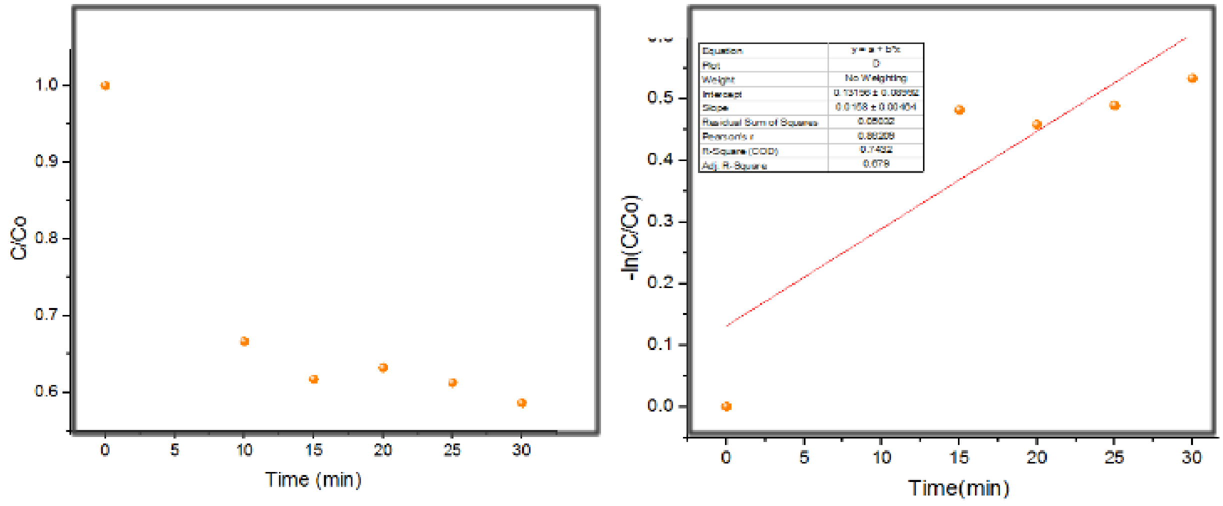

(a)

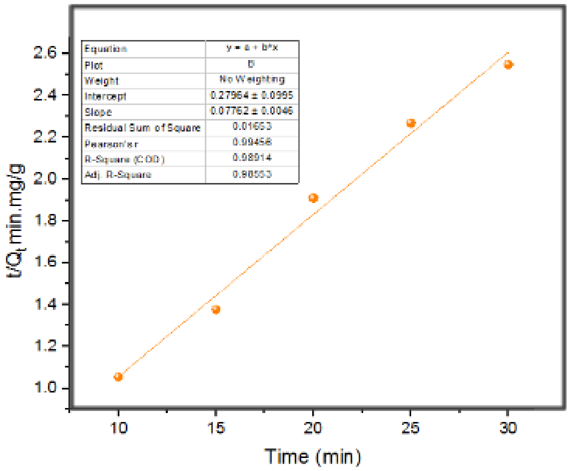

(b)

Fig.46.(a) pseudo first order, (b) pseudo second order

Fig.46.a. represents a pseudo first order kinetic model. The R ² values of the plot are found to be 0.7432. The low values of R ² revealed that the adsorption process may not be well fitted to the pseudo first order adsorption kinetic model.

The fit of t/Qt vs. t with R ² of 0.9891 shows that the adsorption process is well fitted to the pseudo second order adsorption kinetic model.

Kinetic curves for MoSe$_2$

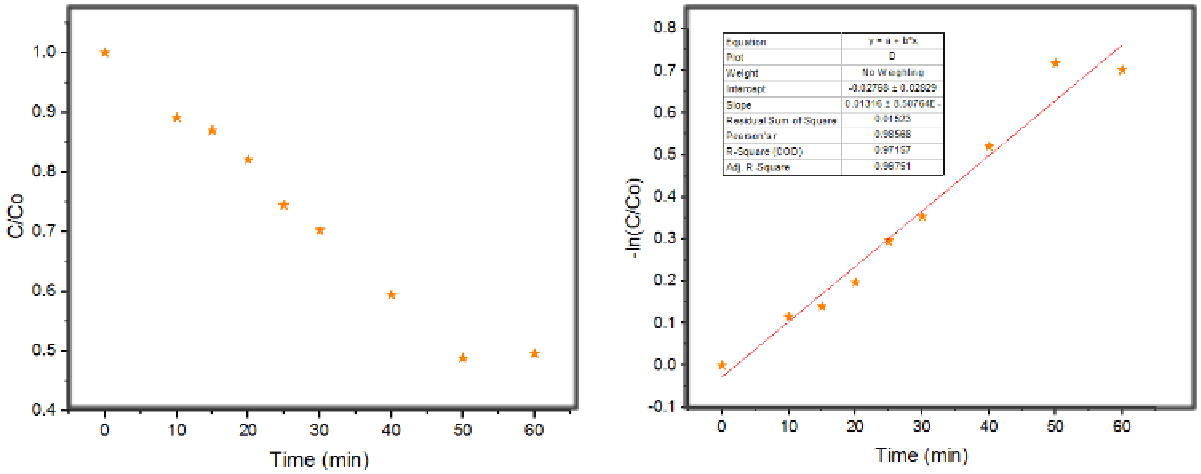

(a) **(b)**

Fig.47:(a)Plot of C/Co vs degradation time for MoSe$_2$ (b) Plot of -ln(C/Co) vs degradation time gives K=0.013/min.

- The wavelength corresponding to maximum absorption of Methyl Orange=464 nm.
- On the addition of MoS_2 to the dye solution the maxima is red shifted to 503 nm while when $MoSe_2$ is added, it shifts to 472 nm.
- Both MoS_2 and $MoSe_2$ show catalytic activity on degradation of Methyl Orange while $MoTe_2$ has no effect on the dye.
- Rate of degradation is found to be higher when MoS_2 is used instead of $MoSe_2$,

SERS Application in the detection of Methyl Orange

Sample preparation and SERS measurements.

100 uL of Gold-nanoparticle solution(10^{-10} M) was mixed with 100 uL of Methyl orange solutions collected at different time intervals after addition of MoS_2. The mixture was then sonicated for 20 min and drop casted on silicon wafers.All samples were analyzed using a LabRAM HR Evol Raman system with a 532 nm laser source. The Raman spectra were collected between 600 and 2000 cm-1.

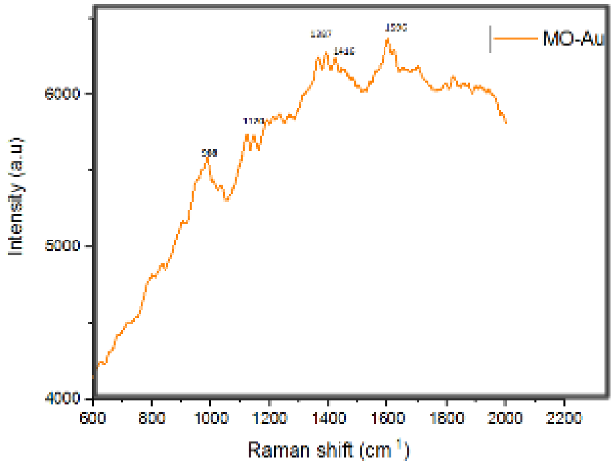

(a)

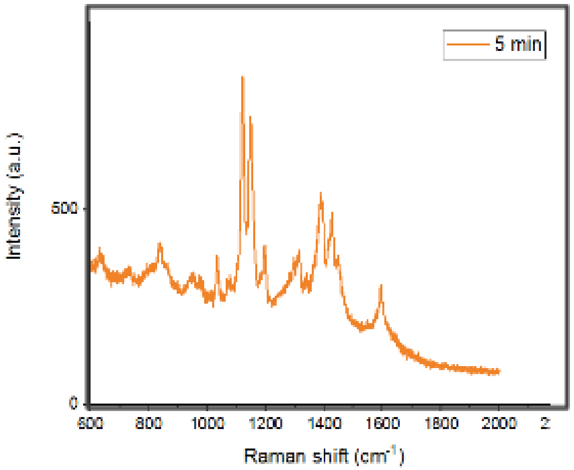

(b)

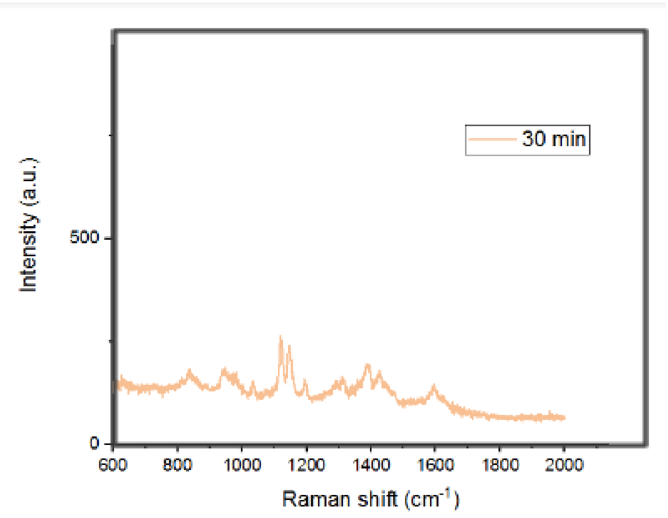

(c)

Fig.48: Raman Spectra: (a)MO-Au (b) 5 min after adding MoS_2 (c) 30 min.

5.10. Catalytic Degradation of dye mixture containing Methyl Orange and Methylene Blue using MoS_2

The activity of the MoS_2 to degrade a mixture of MO and MB was measured by keeping the solution in the dark while it is magnetically being stirred. In this experiment 40 mg of MoS_2 was added to a solution containing 5mL MO (100ppm), 5mL MB (100 ppm) and 90 mL distilled water. The solution was kept in the dark and the concentration of the solution was determined using UV-Visible spectrophotometer.

Fig.49.Degradation of dye mixture containing Methyl Orange and Methylene Blue

- The main absorption edge of Methyl Orange is 464 nm and Methylene Blue is 665 nm.
- The mixture of Methyl orange and Methylene Blue gives a green coloured solution.
- On the addition of MoS_2, the absorption edge of Methyl Orange is red shifted to 500 nm while the absorption edge of Methylene blue remains the same.
- It is noticed from the absorption spectra that MoS2 degrades Methylene Blue first while the change in concentration of Methyl Orange seems negligible.
- Also, the color change from green to orange was observed indicating that most of the methylene blue was already degraded.
- Once methylene blue has almost degraded, degradation of Methyl Orange starts.

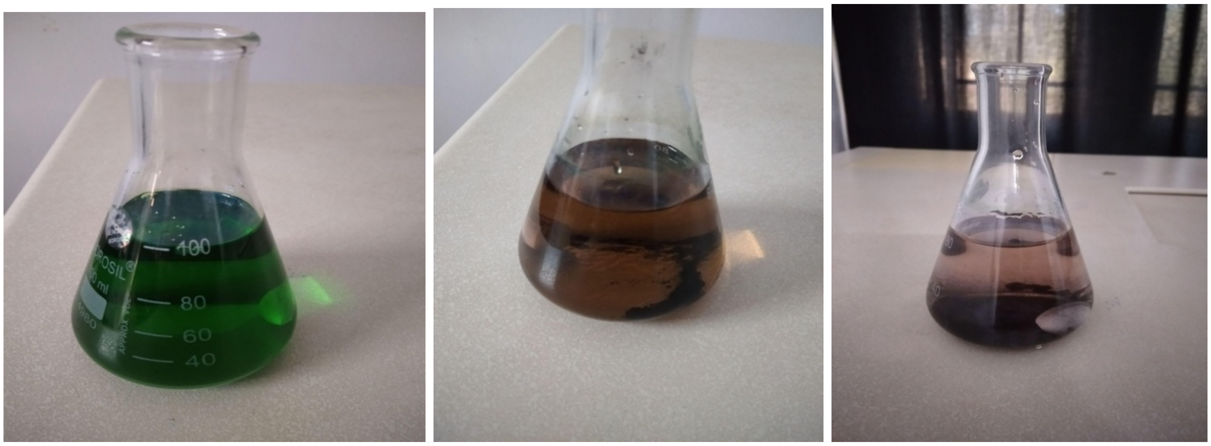
(a) **(b)** **(c)**

Fig.50:(a)Mixture of MO and MB (b) After 55 min of adding MoS_2 (c) After degradation

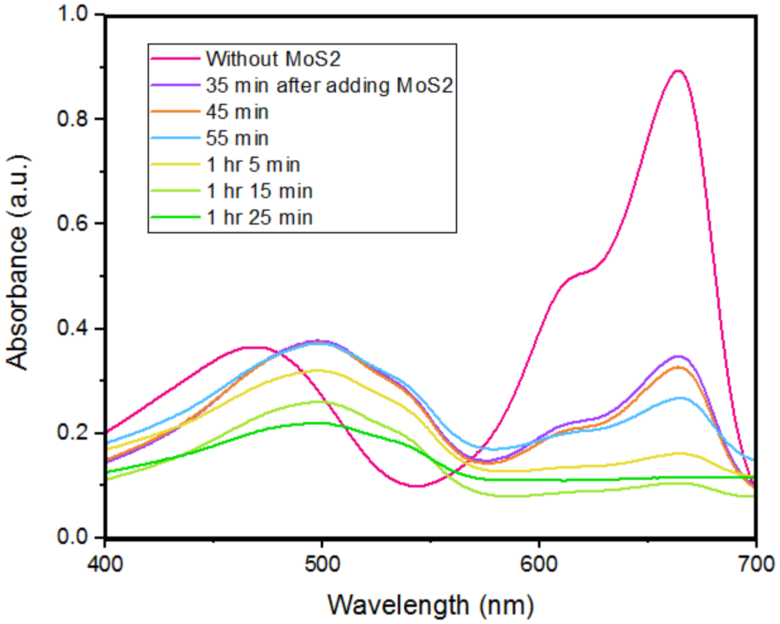

Fig.51. Absorption Spectra for the degradation of dye mixture containing Rhodamine B and Methylene Blue using MoS_2.

5.11.Catalytic Degradation of dye mixture containing Rhodamine B and Methylene Blue

The activity of the MoS_2 nanosheets to degrade a mixture of Rhodamine B and Methylene Blue was measured by keeping the solution in the dark while it is magnetically being stirred. In this experiment 40 mg of MoS_2 nanosheets was added to a solution containing 5mL RhB (100ppm),5mL Methylene Blue (100 ppm) and 90 mL distilled water. The solution was kept in the dark and the concentration of the solution was determined using UV-Visible spectrophotometer.

Fig.52.Catalytic Degradation of dye mixture containing Rhodamine B and Methylene Blue

- The main absorption edge of RhB is 554 nm and Methylene Blue is 665 nm.
- Methylene Blue degrades faster than RhB

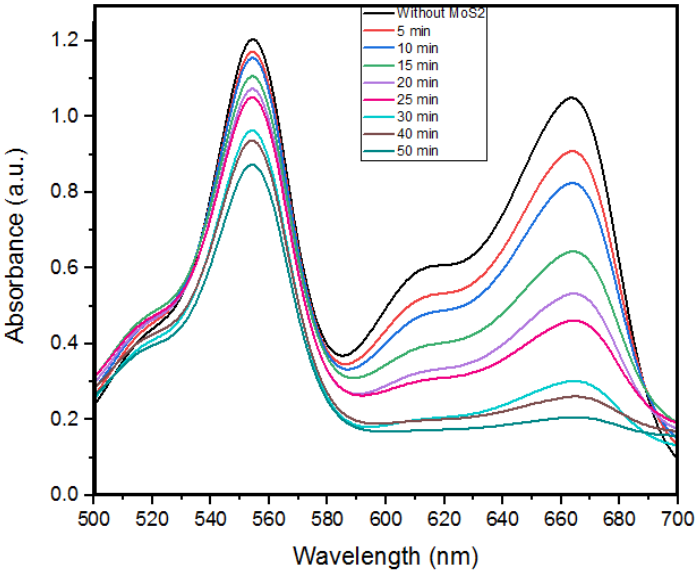

Fig.53. Absorption spectra showing degradation of dye mixture containing RhB and MB.

SERS OF METHYLENE BLUE AND RHODAMINE B MIXTURE

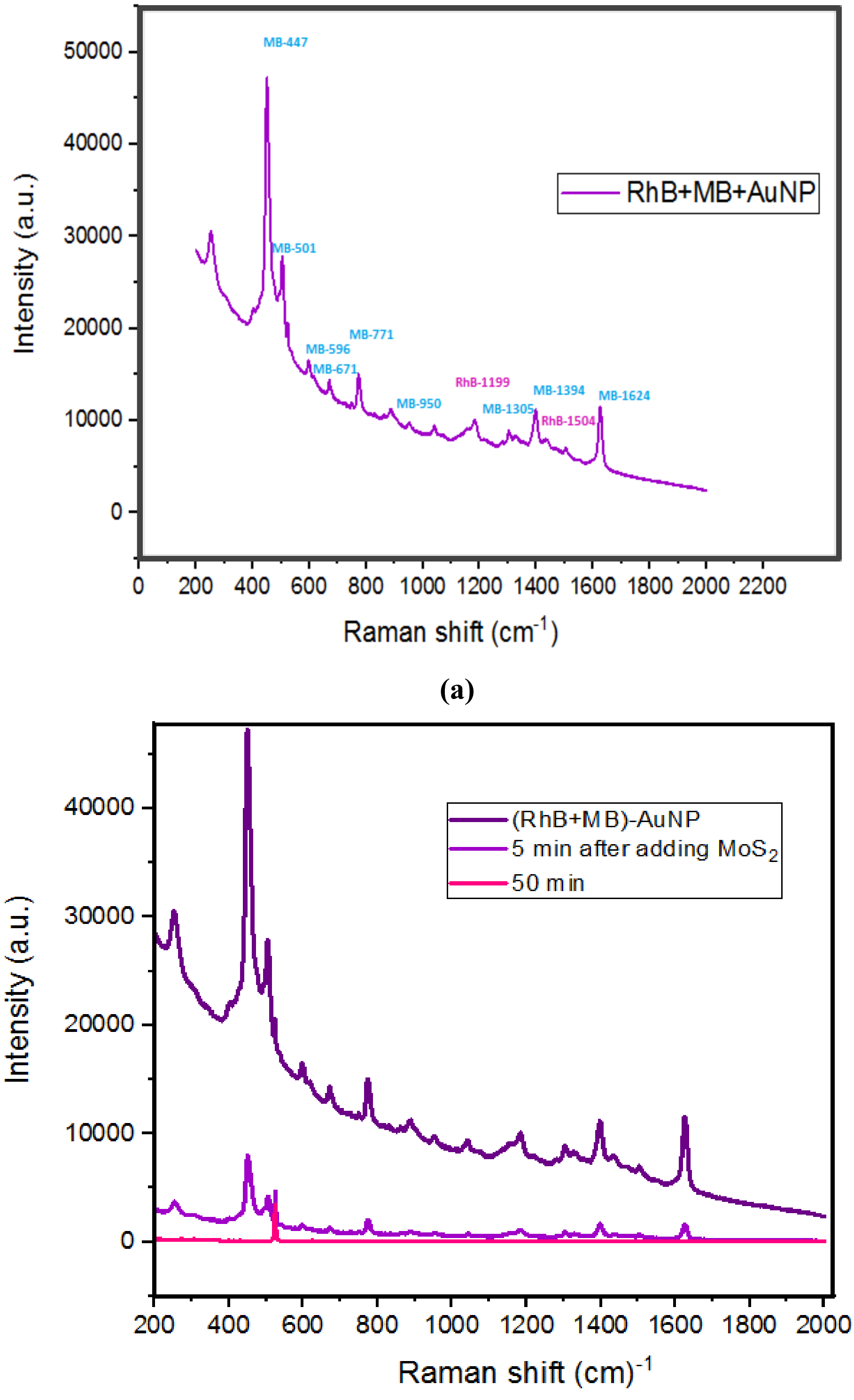

(a)

(b)

Fig.54: Raman Spectra: (a) RhB+MB with AuNP (b)degradation of RhB+MB

5.12.SERS Application in the detection of mixture of Methylene blue and Malachite green

Sample preparation and SERS measurements.

100 uL of Gold-nanoparticle solution(10^{-10} M) was mixed with 100 uL of solution containing a mixture of Malachite Green and Methylene blue (10 mL of 10 ppm each) collected at different time intervals after addition of 40 mg MoS_2. The mixture was then sonicated for 20 min and drop-casted on silicon wafers. All samples were analyzed using a LabRAM HR Evolution Raman system with a 532 nm laser source. The Raman spectra were collected between 200 and 2000 cm-1.

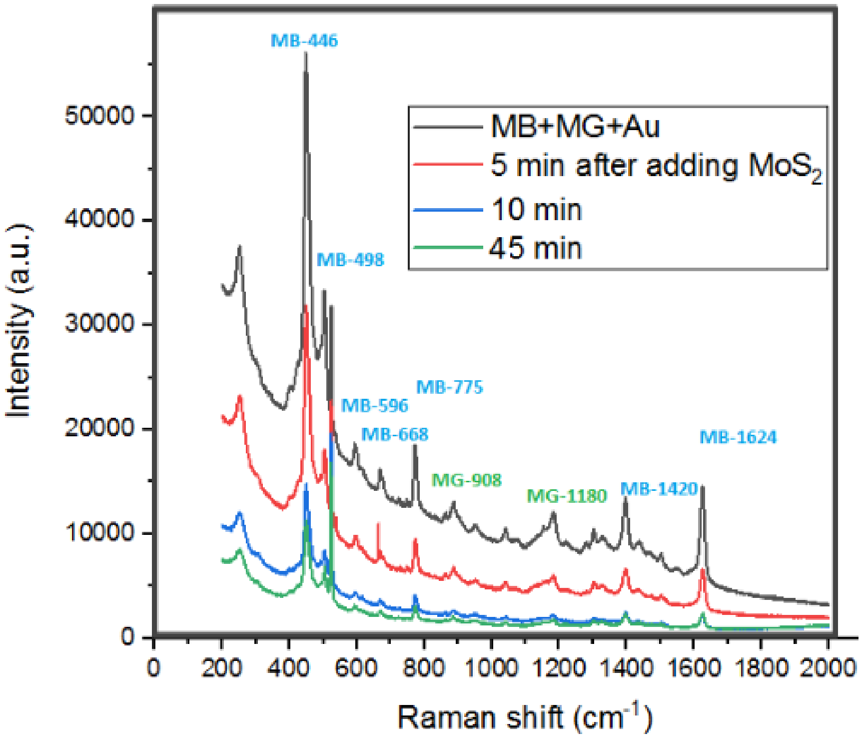

Fig.55. Raman Spectra for degradation of a mixture of Methylene blue and Malachite green

Raman measurements of recovered MoS_2

Recovered MoS_2 after degradation of MB solution was drop-casted on a glass slide containing AuNP. The Raman Spectra shows adsorption of MB onto the surface.

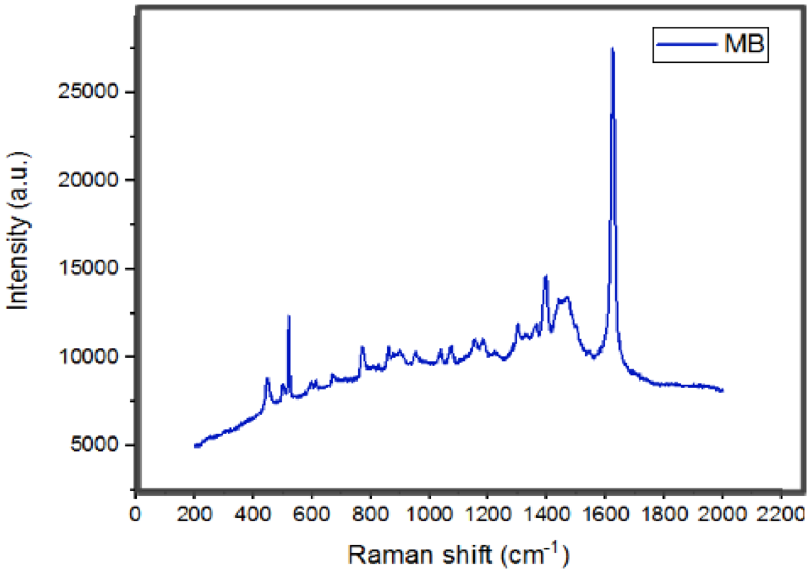

Fig.56. Raman spectra of MB

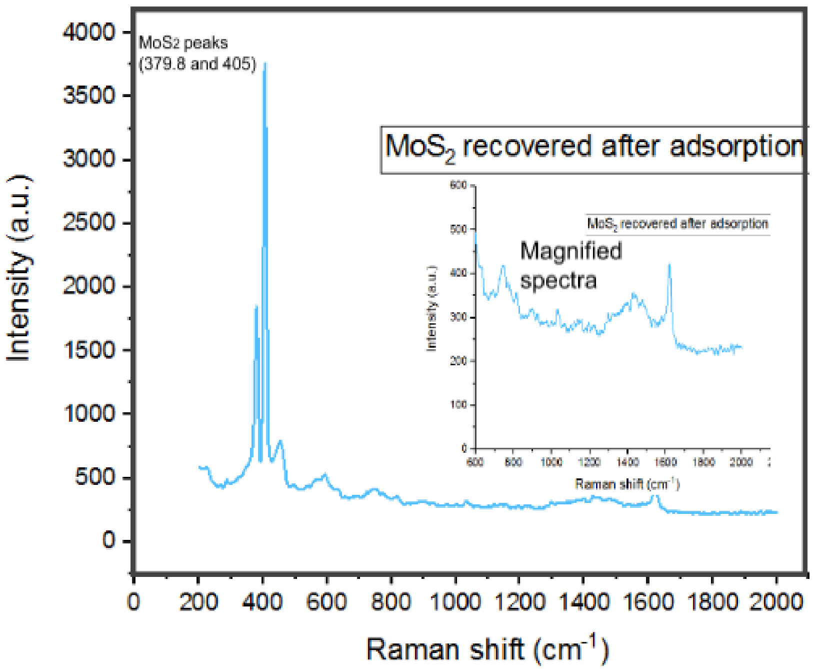

Fig.56.Raman spectra of recovered MoS_2

CHAPTER-6

Conclusion

Conclusion

- In this work, 3D Wurtzite Zinc Selenide (ZnSe) and various Molybdenum Dichalcogenide (MoX_2; X=S, Se, Te) nanostructures have been synthesized using the hydrothermal method.

- The samples were characterized by X-ray diffraction (XRD), Raman Spectroscopy, UV-Visible spectroscopy, Photoluminesence spectroscopy and scanning electron microscopy (SEM).

- The adsorption performance was examined using both cationic and anionic dyes.

- MoS_2 shows remarkable degradation activity of various organic dyes such as MB, MO, MG, Rhodamine B, Rhodamine 6G, mixture of (MO+MB), (MB+MG) and mixture of (MB and RhB) dyes which causes severe environmental contamination issues.

- MoS_2 can be efficiently regenerated and reused for the dye adsorption without compromising the adsorption capacity.

- SERS studies in the detection of dye concentration after regular intervals of time were also performed.

- SERS was performed on the recovered MoS_2 which shows adsorption of MB onto the surface of MoS_2

Future Scope

- Adsorption study of organic dyes on optically trapped MoS_2 surface.
- MoS_2-rGO heterostructure for catalytic degradation of organic dyes.
- To study the reaction mechanism and rate of reaction in combined dye systems.
- Effect of synthesis temperature of MoS_2 on degradation efficiency.
- To study the adsorption isotherm at equilibrium using various isotherm models.
- To investigate whether the adsorption process of the organic dyes is a single layer or multilayer adsorption.
- Effect of temperature and pH on the degradation of combined dye systems.
- Comparative study of MoS_2 vs rGO in the degradation of malachite green.
- Photoluminesence of hydrothermally derived rGO-MoS_2 heterostructures.
- Performance evaluation of MoS_2 nanostructures for hydrogen evolution reaction with different morphology.
- Synthesis and functionalities of MoS_2-borophene heterostructures.
- To study magnetic properties of (MoX_2; X=S, Se, Te)-Fe_3O_4 nanocomposites.

- Synthesis of Au-MoS_2 core-shell heterostructure and its applications in SERS and photoluminescence.

- Development of TMD’s -based devices for energy applications which includes supercapacitors, gas sensors, battery and solar cells.

References:

[1] Gong, Hua & Huang, Hui & Wang, Minqiang & Liu, Kaiping. (2007). Characterization and growth mechanism of ZnSe microspheres prepared by hydrothermal synthesis. Ceramics International. 33. 1381-1384. 10.1016/j.ceramint.2006.03.033.

[2] Lihui, Zhang & Yang, Heqing & yu, Jie & Shao, Fanghong & Li, Li & Zhang, Fenghua & Zhao, Hua. (2009). Controlled Synthesis and Photocatalytic Activity of ZnSe Nanostructured Assemblies with Different Morphologies and Crystalline Phases. Journal of Physical Chemistry C - J PHYS CHEM C. 113. 10.1021/jp810385v.

[3] Feng Cao, Weidong Shi, Lijun Zhao, Shuyan Song, Jianhui Yang, Yongqian Lei, and Hongjie Zhang(2008).Hydrothermal Synthesis and High Photocatalytic Activity of 3D Wurtzite ZnSe Hierarchical Nanostructures.J. Phys. Chem. C 2008, 112, 17095–17101.

[4] Senthilkumar, Kavitha & Thirunavukarasu, Kalaivani & Samikannu, Kanagesan & Balasubramanian, V. & Janarthanan, J.Balakrishnan. (2013). Wurtzite ZnSe quantum dots: Synthesis, characterization and PL properties. Journal of Materials Science Materials in Electronics. 24. 692-696. 10.1007/s10854-012-0796-4.

[5] Xue, S.L. & Wu, S.X. & Zeng, Q.Z. & Xie, P. & Gan, K.X. & Wei, J. & Bu, S.Y. & Ye, X.N. & Xie, L. & Zou, R.J. & Zhang, Chaomin & Zhu, P.F.. (2016). Synthesis, field emission properties and optical properties of ZnSe nanoflowers. Applied Surface Science. 365. 10.1016/j.apsusc.2016.01.022.

[6] FENG S H, XU R R. New materials in hydrothermal synthesis [J]. Accounts Chem Res, 2001, 34(3): 239−247.

[7] CAO F, SHI W D, ZHAO L J, SONG S Y, YANG J H, LEI Y Q, ZHANG H J. Hydrothermal synthesis and high photocatalytic activity of 3D wurtzite ZnSe hierarchical nanostructures [J]. J Phys Chem C, 2008, 112(44): 17095−17101.

[8] Karthik S.Bhat,H.S.Nagaraja.Performance evaluation of molybdenum dichalcogenide (MoX2;X=S,Se,Te) nanostructures for hydrogen evolution reaction.International Journal of Hydrogen Energy.

[9] S. J. Sandoval, D. Yang, R. F. Frindt, and J. C. Irwin, Phys. Rev. B 44, 3955–3962 (1991).

[10] Lee JH, Gul HZ, Kim H, Moon BH, Adhikari S, Kim JH et al (2017) Photocurrent switching of monolayer MoS2 using a metal-insulator transition. Nano Lett 17:673–678.

[11] Kim T, Mun J, Park H, Joung D, Diware M, Won C et al (2017) Wafer-scale production of highly uniform two-dimensional MoS2 by metal-organic chemical vapor deposition. Nanotechnology 28:18LT01.

[12] Singh E, Kim KS, Yeom GY, Nalwa HS (2017) Atomically thin-layered molybdenum disulfide (MoS2) for bulk-heterojunction solar cells. ACS Appl Mater Interfaces 9:3223–3245.

[13] Ghaleghafi, Elahe & Rahmani, Mohammad Bagher & Wei, Zung-Hang. (2021). Photoluminescence and UV photosensitivity of few-layered MoS2 nanosheets synthesized under different hydrothermal growth times. Journal of Materials Science. 56. 10.1007/s10853-021-06083-x.

[14] Hussain, Sajjad & Patil, Dr. Supriya & Vikraman, Dhanasekaran & Mengal, Naveed & Liu, Hailiang & Song, Wooseok & An, Ki-Seok & Jeong, Sung & Kim, Hun-Sung & Jung, Jongwan. (2018). Large area growth of MoTe2 films as high performance counter electrodes for dye-sensitized solar cells. Scientific Reports. 8. 10.1038/s41598-017-18067-6.

[15] Wang, Kai & Wu, Jie & Chen, Gexiang & Qiao, Hui & Zhou, Yang & Li, Jun & Qi, Xiang. (2021). A Robust 3D Self-powered Photoelectrochemical type Photodetector based on MoSe2 Nanoflower. 10.21203/rs.3.rs-343198/v1.

[16] Massey, Anushka & Gusain, Rashi & Kumari, Sangita & Khatri, Om. (2016). Hierarchical Microspheres of MoS2 Nanosheets: Efficient and Regenerative Adsorbent for Removal of

Water-Soluble Dyes. Industrial & Engineering Chemistry Research. 55. 10.1021/acs.iecr.6b01115.

[17] Singh, Jaspal & Rishikesh, & Kumar, Sanjeev & Soni, Ravi. (2020). Synthesis of 3D-MoS2 nanoflowers with tunable surface area for the application in photocatalysis and SERS based sensing. Journal of Alloys and Compounds. 849. 156502. 10.1016/j.jallcom.2020.156502.

[18] Wang, X.; Ding, J.; Yao, S.; Wu, X.; Feng, Q.; Wang, Z.; Geng, B. High
Supercapacitor and Adsorption Behaviors of Flower-Like MoS2 Nanostructures. J. Mater. Chem

[19] Wu, Yanhong & Su, Minhua & Chen, Jiawei & Xu, Zuopeng & Tang, Jiafeng & Chang, Xiangyang & Chen, Diyun. (2019). Superior adsorption of methyl orange by h-MoS2 microspheres: Isotherm, kinetics, and thermodynamic studies. Dyes and Pigments. 170. 107591. 10.1016/j.dyepig.2019.107591.

[20] Yang, Guijun & Park, Soo-Jin. (2019). Conventional and Microwave Hydrothermal Synthesis and Application of Functional Materials: A Review. Materials. 12. 1177. 10.3390/ma12071177.

[21] Yagub, M. T.; Sen, T. K.; Afroze, S.; Ang, H. M. Dye and Its Removal from Aqueous
Solution by Adsorption: A Review. Adv. Colloid Interface Sci. 2014, 209, 172.

[22] Xiao Xia Han,Rebeca S.Rodriguez,Christy L. Haynes, Yukihiro Ozaki and Bing Zhao. Surface-enhanced Raman spectroscopy.Nature reviews(2021)1:87.

[23] Khataee, Alireza & Kasiri, Masoud. (2010). Photocatalytic degradation of organic dyes in the presence of nanostructured titanium dioxide: Influence of the chemical structure of dyes. Journal of Molecular Catalysis A: Chemical. 328. 8–26. 10.1016/j.molcata.2010.05.023.

[24] Yu, Yifu & Nam, Gwang-Hyeon & He, Qiyuan & Wu, Xue-Jun & Zhang, Kang & Yang, Zhenzhong & Junze, Chen & Ma, Qinglang & Zhao, Meiting & Liu, Zhengqing & Ran,

Fei-Rong & Wang, Xingzhi & Li, Hai & Huang, Xiao & Li, Bing & Xiong, Qihua & Zhang, Qing & Liu, Zheng & Gu, Lin & Zhang, Hua. (2018). High phase-purity 1T'-MoS2- and 1T'-MoSe2-layered crystals. Nature chemistry. 10. 10.1038/s41557-018-0035-6.